

Radiation boundary conditions for the numerical simulation of waves

Thomas Hagstrom*

Department of Mathematics and Statistics,

The University of New Mexico,

Albuquerque, NM 87131, USA

E-mail: hagstrom@math.unm.edu

We consider the efficient evaluation of accurate radiation boundary conditions for time domain simulations of wave propagation on unbounded spatial domains. This issue has long been a primary stumbling block for the reliable solution of this important class of problems. In recent years, a number of new approaches have been introduced which have radically changed the situation. These include methods for the fast evaluation of the exact nonlocal operators in special geometries, novel sponge layers with reflectionless interfaces, and improved techniques for applying sequences of approximate conditions to higher order. For the primary isotropic, constant coefficient equations of wave theory, these new developments provide an essentially complete solution of the numerical radiation condition problem.

In this paper the theory of exact boundary conditions for constant coefficient time-dependent problems is developed in detail, with many examples from physical applications. The theory is used to motivate various approximations and to establish error estimates. Complexity estimates are also derived to compare different accurate treatments, and an illustrative numerical example is given. We close with a discussion of some important problems that remain open.

* Supported, in part, by NSF Grant DMS-9600146, the Institute for Computational Mechanics in Propulsion (ICOMP), NASA, Lewis Research Center, Cleveland, Ohio; DARPA/AFOSR Contract F49620-95-C-0075; and, while in residence at the Courant Institute, DOE Contract DEFGO288ER25053.

CONTENTS

1	Introduction	48
2	Formulations of exact boundary conditions	50
3	Approximations and implementations	76
4	Conclusions and open problems	100
	References	103

1. Introduction

Problems in wave propagation have played and will continue to play a central role in the mathematical analysis of physical and biological systems. A defining feature of most wave problems is the radiation of energy to the far field. Mathematically, this is naturally modelled by the use of an unbounded domain, with the addition, in frequency domain problems, of a radiation boundary condition at infinity. In numerical simulations, the accurate approximation of radiation to the far field is also crucial. As it is impossible to solve directly a problem posed on an unbounded domain, new techniques, such as the introduction of an artificial boundary and associated radiation boundary conditions, are needed. The goal of this article is to outline the development, implementation, and analysis of various practical methods for solving this problem for some important models, and to present what I believe is a useful mathematical framework in which to pursue improvements and extensions.

Although wave propagation is inherently a time-dependent phenomenon, it has been fruitful in many settings to solve linear problems in the frequency domain. Approaches to the accurate solution of elliptic boundary value problems on unbounded domains are, generally, far better developed than their time domain analogues. Useful techniques include a variety of boundary integral methods, which may be applied on physical or artificial boundaries, including classical integral equations of potential theory (Greengard and Rokhlin 1997, Rokhlin 1990), extensions of Calderon–Seeley equations (Ryabeńkii 1985), the Dirichlet-to-Neumann map (Givoli 1992) and infinite elements (Bettess 1992, Demkowicz and Gerdes 1999). Moreover, the efficiency of solving the classical equations has been greatly enhanced in the past decade through the introduction of the fast multipole method.

The aims of the numerical analysis of partial differential equations on unbounded domains are clear. We seek methods which:

- (i) can automatically achieve any prescribed accuracy on bounded subsets of the original domain,
- (ii) in terms of both computation and storage, cost no more than the solution of a standard problem on the bounded subdomain.

Though certainly more research and development is called for, it is my opinion that these goals have been or can be met by the methods mentioned above for most elliptic problems. An exception to this is the difficult case of Helmholtz-type equations with general variable coefficients at infinity.

The situation with time-dependent problems has been far less satisfactory. The general belief was that exact domain reductions, which necessarily involve history-dependent operators, could never be made computationally feasible. As a result, various simple approximations were employed. These easily met the second criterion, but their accuracy was often poorly understood. Although the approximate conditions proposed were typically embedded in a hierarchy of conditions of increasing order and, presumably, accuracy, as in Lindman (1975), Engquist and Majda (1977, 1979), and Bayliss and Turkel (1980), the hierarchy was rarely used. For some problems it seemed that good results were obtained with the low-order approximations. However, there was generally no way to monitor or decrease the error automatically. Moreover, as we shall see later, it is possible to pose very simple problems for which the standard methods produce inaccurate results. Clearly, our first criterion is not met by the simpler techniques, which from the point of view of the numerical analyst is completely unacceptable.

In the past few years, the situation has radically changed, at least for the basic, constant coefficient equations of wave theory. Progress has been made on many fronts, including:

- (i) the development of efficient algorithms for evaluating exact, temporally nonlocal boundary operators through the use of exact or uniformly accurate rational representations of the transforms of their associated convolution kernels,
- (ii) the development of improved sponge layer techniques exhibiting reflectionless interfaces with the lossless interior domains,
- (iii) improved techniques for the implementation to higher orders of the older hierarchies of approximate conditions, along with improvements in the analysis of their convergence with increasing order.

In this article, I hope to give a broad exposition from a unified viewpoint of the developments listed above. The reader should be cautioned from the outset that, in comparison with typical theories in computational mathematics, what follows may seem rather specialized. We deal with special equations, often restrict ourselves to special boundaries, and make use of special functions. That said, the results themselves have enormous applicability as the equations we can successfully treat include many of the most important in applications. Moreover, it is not unreasonable to hope that some of these methods will be generalizable to problems we cannot now solve.

Our approach to the theory of radiation boundary conditions is straightforward. First, we construct exact boundary conditions. Although such conditions can be described in some generality as certain projections of boundary data, we concentrate on concrete expressions derived by separation of variables. For artificial boundaries that satisfy a scale invariance condition, the exact condition factors into the composition of nonlocal spatial and temporal operators. Approximate conditions are analysed using the standard concepts: stability and consistency. From this analysis we obtain sharp error estimates for a wide variety of techniques. These error bounds are used to estimate the computational complexity of the competing methods. The results are also illustrated by a simple numerical experiment. It should be noted that a comprehensive body of numerical results on an appropriate set of benchmark problems is lacking. There has been interest in developing such a set (see Geers (1998)), and I am of the opinion that the problems used here and in Alpert, Greengard and Hagstrom (1999a) and Hagstrom and Goodrich (1998) are particularly useful, due both to the simplicity of their definition and to the difficulty of their solution.

What I have not tried to do is give a comprehensive survey of the many contributions to this subject that have appeared over the past twenty years. The reader is referred to the survey articles (Givoli 1991, Tsynkov 1998) which have extensive bibliographies. I do make many references to the literature within the text, but these are primarily intended to aid the reader who wishes to delve into the subject more deeply, rather than to provide an accurate historical record of its development.

Finally I would like to acknowledge the important contributions of those who collaborated with me on a variety of research projects in this field: Brad Alpert, John Goodrich, Leslie Greengard, S. I. Hariharan, H. B. Keller, Jens Lorenz, Richard MacCamy, Jan Nordström, and Liyang Xu. I also acknowledge the support of the NSF, the Institute for Computational Mechanics in Propulsion (NASA), DARPA/AFOSR, and, for work done while in residence at the Courant Institute, DOE. Throughout I have tried to emphasize the personal nature of the conclusions expressed herein through the use of the first person, and take full responsibility for them.

2. Formulations of exact boundary conditions

In this section I briefly develop the theory of exact boundary conditions for time-dependent problems and apply it to derive explicit expressions for a long list of problems with simple artificial boundaries. The list includes the scalar wave equation and its dispersive analogue, Maxwell's equations, the linear elasticity equations, the advection-diffusion equation, the Schrödinger equation, the linearized compressible Euler equations, and the linearized incompressible Navier-Stokes equations. My purpose in presenting so many

examples, aside from the inherent physical interest in all of them, is to demonstrate the remarkable unity of the problem. In particular, although the details of each calculation differ, the recipe for carrying them out does not. Moreover, we shall see that the same few convolution kernels reappear in example after example to define the temporally nonlocal part of the exact condition. Practically, this means that the accurate approximation or compression of a rather small number of operators will have extensive applications. I will show how this can be done in the second part of this article.

The outline of the theory of exact conditions presented here has been known for some time (Gustafsson and Kreiss 1979, Hagstrom 1983). However, it was only recently used to develop and analyse efficiently implementable but arbitrarily accurate approximations. The equations considered fall into two classes: hyperbolic equations for which the spatial and temporal operators have the same order, and equations which are first order in time but second order in space. Viewed as pseudodifferential operators, the exact conditions in each case are of different types. As a result our techniques for separating them into local and nonlocal parts differ.

2.1. The scalar wave equation

The scalar wave equation is the most ubiquitous model of wave propagation and, hence, is the natural starting point for our study. Consequently, the vast majority of work on the subject has been devoted to this case. I will proceed from the general to the particular, ending with useful expressions for exact conditions on planar, spherical and cylindrical artificial boundaries.

General boundaries

We consider a mixed problem for the inhomogeneous wave equation in an unbounded domain, Ω :

$$\frac{\partial^2 u}{\partial t^2} = c^2 \nabla^2 u + f, \quad t > 0, \quad x \in \Omega, \quad (2.1)$$

with initial and boundary conditions:

$$u(x, 0) = u_0(x), \quad \frac{\partial u}{\partial t}(x, 0) = v_0(x), \quad (2.2)$$

$$\alpha \frac{\partial u}{\partial n} + \beta \frac{\partial u}{\partial t} + \gamma u = g, \quad x \in \partial\Omega. \quad (2.3)$$

To truncate the problem, we choose a bounded subdomain, $\Upsilon \subset \Omega$, which we assume contains the support of the data, f , u_0 , v_0 and g . The boundary of Υ then consists of two parts, $\Sigma \subset \partial\Omega$ and what we will call the *artificial boundary*, Γ . For example, if we are solving an exterior problem, that is, if

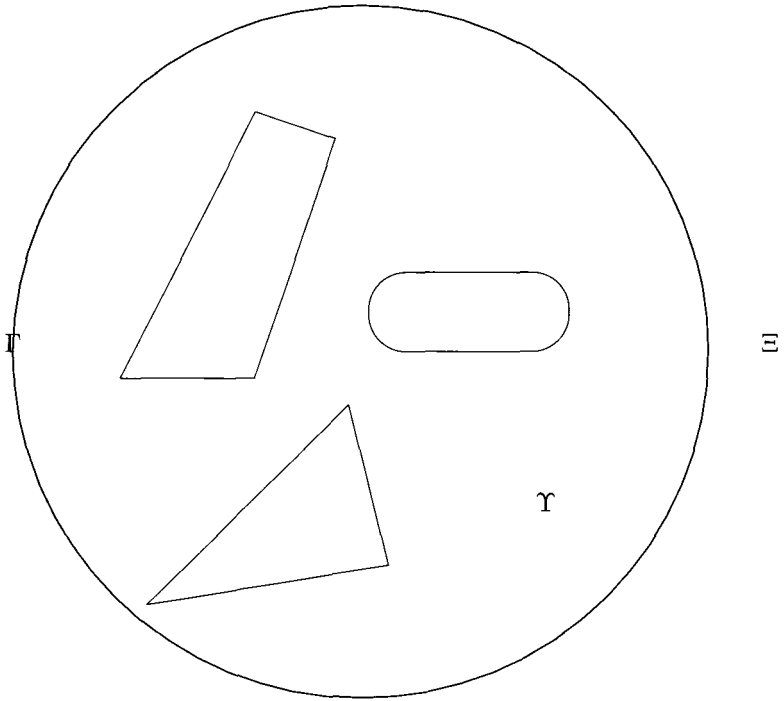


Fig. 1. Domains for an exterior problem: Ξ is the tail, Υ is the computational domain, Γ is the artificial boundary

the domain Ω is the complement of some finite number of finite domains, then Σ will consist of the boundaries of these regions while Γ will be some closed surface which surrounds them. (See Figure 1.)

In Υ we solve (2.1), (2.2) and (2.3) supplemented by an additional boundary condition on Γ :

$$B_e u = 0, \quad x \in \Gamma. \quad (2.4)$$

We term the boundary condition (2.4) *exact* if the truncated problem has a unique solution which, for all $t > 0$, coincides with the restriction to Υ of the solution of the original problem posed on the unbounded domain Ω . Note that we insist on a homogeneous boundary condition on Γ , so that it will be explicitly independent of the data. If we allowed the support of these to extend beyond Υ an inhomogeneous condition would generally be required.

An indirect description of B_e may be derived as follows. Consider the part of the domain 'discarded' as we pass from Ω to Υ , *i.e.*, the 'tail', $\Xi = \Omega - \Upsilon$. Consider the set, \mathcal{S} , consisting of all solutions of the homogeneous wave equation in Ξ , with zero initial data and satisfying the boundary condition (2.3) with $g = 0$ on that part of $\partial\Xi$ which is also part of $\partial\Omega$. As we have as yet imposed no boundary condition on Γ , we expect that \mathcal{S} will be infinite.

Now the restriction to Ξ from Ω of the solution, u , to our original problem must be an element of \mathcal{S} . Moreover, so long as the trace on Γ of a solution of (2.1), (2.2), (2.3) in Υ , along with the trace of its normal derivative, coincide with the traces of an element, w , of \mathcal{S} , the solution is easily extended to Ω by simply setting it equal to w in Ξ . Set \mathcal{A} to be the linear subspace of all pairs of functions on Γ which coincide with the trace of an element of \mathcal{S} and the trace of its normal derivative. We call \mathcal{A} the *admissible subspace*. Then B_e is defined by

$$B_e u = 0 \iff u \in \mathcal{A}.$$

More directly, this formulation represents $B_e = I - P_{\mathcal{A}}$, where $P_{\mathcal{A}}$ is a projection operator for \mathcal{A} . We have been somewhat informal in our use of concepts from functional analysis, and the full justification of this abstract construction requires more work. However, the general recipe outlined here may be applied to other problems, as will be shown below. It also forms the basis of the construction of exact conditions for elliptic problems as given in Hagstrom and Keller (1986).

Useful, and generally easily justifiable, representations of the operator B_e can be obtained by means of Laplace transformation and the theory of elliptic equations. We thus consider the Helmholtz equation

$$\tilde{s}^2 \hat{u} = \nabla^2 \hat{u}, \quad x \in \Xi, \tag{2.5}$$

with boundary conditions

$$\alpha \frac{\partial \hat{u}}{\partial n} + (s\beta + \gamma) \hat{u} = 0, \quad x \in \partial\Omega \cap \partial\Xi, \tag{2.6}$$

and s restricted to some right half-plane,

$$\operatorname{Re} s \geq \eta \geq 0. \tag{2.7}$$

We have also introduced

$$\tilde{s} = \frac{s}{c}.$$

At least for η sufficiently large, we also require that \hat{u} be bounded and assume that α, β, γ are real and

$$\alpha, \beta \geq 0.$$

For our purposes, it is simplest to parametrize the transforms of elements of \mathcal{S} by their boundary values at Γ . In particular, given some sufficiently smooth function $\hat{w}(x, s)$ defined on Γ , there exists a unique solution, \hat{u} , of (2.5)–(2.6) such that

$$\hat{u}(x, s) = \hat{w}(x, s), \quad x \in \Gamma.$$

See, for instance, Ramm (1986) for proofs in various unbounded domains. Now we may compute the trace of the normal derivative (outward for Υ) of

this solution on Γ , which defines the so-called Dirichlet-to-Neumann map, $-\hat{\mathcal{D}}$:

$$\frac{\partial \hat{u}}{\partial n} = -\hat{\mathcal{D}}\hat{w}, \quad x \in \Gamma.$$

Denoting Laplace transformation by \mathcal{L} , our exact boundary operator B_e may thus be defined by

$$B_e u \equiv \frac{\partial u}{\partial n} + \mathcal{L}^{-1} \left(\hat{\mathcal{D}} \mathcal{L} u \right). \quad (2.8)$$

We note that B_e is not a local (*i.e.*, differential) operator. This fact has led to the conclusion that direct implementations of the exact condition are uneconomical: a conclusion we shall demonstrate to be false for some special choices of the artificial boundary.

One way to express $\hat{\mathcal{D}}$ is in terms of the Green's function for the problem in Ξ . Let $G(x, y, s)$ satisfy

$$\left(\nabla_y^2 - s^2 \right) G = \delta(x - y),$$

along with (2.6) (in y) and

$$G = 0, \quad y \in \Gamma.$$

Then, for $x \in \Gamma$,

$$-\hat{\mathcal{D}}w(x) = -\frac{\partial}{\partial n_x} \int_{\Gamma} \frac{\partial G}{\partial n_y}(x, y, s) w(y) dy.$$

(This equation must be interpreted in terms of limits as $x \rightarrow \Gamma$.)

For purposes of computation, it is most convenient to express $\hat{\mathcal{D}}$ in terms of its eigenvalues and eigenfunctions, that is,

$$\hat{\mathcal{D}}\hat{w}(y, s) = \sum_{j=1}^{\infty} \lambda_j(s) Y_j(y, s) \int_{\Gamma} Y_j^*(z, s) \hat{w}(z, s) dz.$$

In special cases this representation further simplifies, as the eigenfunctions, Y_j , turn out to be independent of s . Then the nonlocality may be expressed as the composition of a spatial and temporal operator, each of which may be amenable to a 'fast' evaluation. The invariance of the eigenfunctions with s follows from a scale invariance of the artificial boundary. Boundaries for which it holds include planes, spheres, cylinders and cones. Detailed expressions for B_e in these cases are developed below.

We finally note that extensions of the solution in Ξ from Γ to another boundary $\Gamma' \subset \Xi$ may be used in lieu of the exact boundary condition. Precisely, it follows from causality that for any $x' \in \Gamma'$ we may derive rep-

representations of the form

$$u(x', t') = \int_{t < t' - \delta/c} \int_{\Gamma} \left(K_D(x', x, t', t)u(x, t) + K_N(x', x, t', t) \frac{\partial u}{\partial n}(x, t) + K_T(x', x, t', t) \frac{\partial u}{\partial t}(x, t) \right) dx dt, \tag{2.9}$$

where the kernels $K_{D,N,T}$ are determined by the geometry of Ξ and the choice of Γ' and where δ is the minimum distance between the two boundaries. Indeed, such expressions follow from the various representations of solutions of (2.5) by potential theory. Using (2.9) to provide Dirichlet data at Γ' , it is possible to solve the wave equation in the extended domain consisting of the union of Υ and that part of Ξ bounded by Γ and Γ' . This approach was first suggested by Ting and Miksis (1986) and later implemented by Givoli and Kohen (1995) for exterior problems in three space dimensions. Then one may use the well-known Kirchoff formula as a particular realization of (2.9):

$$u(x', t') = -\frac{1}{4\pi} \int_{\Gamma} \left(\frac{\partial}{\partial n} \left(\frac{1}{r} \right) \cdot u(x, t - r/c) - \frac{1}{r} \frac{\partial u}{\partial n}(x, t - r/c) - \frac{1}{rc} \frac{\partial r}{\partial n} \frac{\partial u}{\partial t}(x, t - r/c) \right) dx,$$

where $\partial/\partial n$ is the outward normal derivative on Γ and

$$r = |x - x'|.$$

Although I do not expect that boundary conditions based on this formula will be competitive from the point of view of cost with other equally accurate treatments discussed below, it is important to note that the paper of Ting and Miksis (1986) represents one of the first serious attempts to use exact conditions for the time-dependent wave equation. It is generalized to the equations of elasticity in Givoli and Kohen (1995) and to Maxwell's equations in He and Weston (1996).

Planar boundary

We now suppose that Ξ consists of the half-space $(x, y) \in (0, \infty) \times R^{n-1}$. Applying a Fourier transformation in y with dual variables k , (2.5) becomes the ordinary differential equation

$$\frac{\partial^2 \hat{u}}{\partial x^2} = (\tilde{s}^2 + |k|^2) \hat{u}, \quad x > 0. \tag{2.10}$$

For $\text{Re } s > 0$, bounded solutions of (2.10) are of the form

$$A(s, k)e^{-(\tilde{s}^2 + |k|^2)^{1/2}x},$$

where the branch of $\hat{\mathcal{D}} = (\tilde{s}^2 + |k|^2)^{1/2} \equiv \sqrt{\tilde{s}^2 + |k|^2}$ is chosen so that $\hat{\mathcal{D}}$ is analytic and has positive real part when $\text{Re } \tilde{s} > 0$ and satisfies

$$\hat{\mathcal{D}} \sim \tilde{s}, \quad \tilde{s} \rightarrow \infty.$$

The branch cut is conveniently chosen to be a curve in $\text{Re } \tilde{s} < 0$ connecting the branch points $\pm i|k|$.

The exact condition (2.8) is expressed in terms of u in the following way. Let \mathcal{F} denote Fourier transformation with respect to y , and let \mathcal{F}^{-1} be its inverse. Rewrite $\hat{\mathcal{D}}$ by removing its large \tilde{s} part so that the remainder is the transform of a function

$$\hat{\mathcal{D}} = \tilde{s} + \left(\sqrt{\tilde{s}^2 + |k|^2} - \tilde{s} \right).$$

Finally, let

$$K(t) = \frac{J_1(t)}{t} = \frac{1}{\pi} \int_{-1}^1 \sqrt{1-w^2} \cos wt \, dw. \quad (2.11)$$

As shown, for example, in Hagstrom (1996),

$$\hat{K}(s) = \sqrt{s^2 + 1} - s.$$

Therefore, using standard formulas from Laplace transform theory (e.g., Doetsch (1974)) we finally have the exact condition at $x = 0$:

$$\frac{\partial u}{\partial x} + \frac{1}{c} \frac{\partial u}{\partial t} + \mathcal{F}^{-1} \left(c|k|^2 K(c|k|t) * (\mathcal{F}u) \right) = 0. \quad (2.12)$$

(Here, $*$ denotes convolution in time.)

Note that, as mentioned in the preceding section, we have written B_e as the composition of nonlocal spatial and temporal operators. This is a consequence of the fact that the eigenfunctions of $\hat{\mathcal{D}}$ are simply the Fourier modes and, hence, are independent of s .

We note that the exact condition (2.12) applies with minor modification to problems that are periodic in y or that are posed in cylindrical domains such as waveguides. Indeed, it even applies to certain problems with variable coefficients. Consider

$$\frac{\partial^2 u}{\partial t^2} = c^2 \left(\frac{\partial^2 u}{\partial x^2} + Lu \right), \quad (x, y) \in (0, \infty) \times \Theta \equiv \Xi,$$

with some homogeneous boundary conditions, $B_s u = 0$, $y \in \partial\Theta$. Suppose, with these boundary conditions, that the operator L has a complete, L_2 -orthonormal set of eigenfunctions $Y_j(y)$ with negative, real eigenvalues $-\kappa_j^2$. For example, L could be a variable coefficient Sturm–Liouville operator. Then the analysis above can be repeated with the Fourier transform replaced

by the Sturm–Liouville expansion and $|k|$ replaced by κ_j . Precisely, we have

$$\frac{\partial u}{\partial x} + \frac{1}{c} \frac{\partial u}{\partial t} + \sum_{j=1}^{\infty} Y_j(y) \left(c\kappa_j^2 K(c\kappa_j t) * \left(\int_{\Theta} Y_j(y') u(0, y', t) dy' \right) \right) = 0. \quad (2.13)$$

Spherical boundary

Using standard spherical coordinates, (ρ, θ, ϕ) , Ξ is defined by $\rho > R$ and Γ is the sphere $\rho = R$. The Laplace transform of the solution, \hat{u} , in the tail is now expanded in spherical harmonics, that is,

$$\hat{u}(\rho, \theta, \phi, s) = \sum_l \hat{u}_l Y_l(\theta, \phi),$$

where

$$\nabla_{\text{sphere}}^2 Y_l = -l(l+1)Y_l,$$

and

$$\frac{\partial^2 \hat{u}_l}{\partial \rho^2} + \frac{2}{\rho} \frac{\partial \hat{u}_l}{\partial \rho} - \left(\tilde{s}^2 + \frac{l(l+1)}{\rho^2} \right) \hat{u}_l = 0. \quad (2.14)$$

For $\text{Re } s > 0$, bounded solutions of (2.14) in Ξ are given by

$$\hat{u}_l = A_l(\tilde{s}) \sqrt{\frac{\pi}{2\rho\tilde{s}}} K_{l+1/2}(\rho\tilde{s}),$$

the modified spherical Bessel function of the third kind. (See Abramowitz and Stegun (1972, Ch. 10).) It may be represented in terms of elementary functions:

$$\sqrt{\frac{\pi}{2z}} K_{l+1/2}(z) \equiv k_l(z) = \frac{\pi}{2z} e^{-z} \sum_{k=0}^l \frac{(l+k)!}{k!(l-k)!} (2z)^{-k}. \quad (2.15)$$

Hence we have the following expression for the exact boundary condition, which as before we write as the sum of a local operator and convolution with a function

$$\hat{\mathcal{D}}_l = - \left(\frac{((R\tilde{s})^{-1/2} K_{l+1/2}(R\tilde{s}))'}{(R\tilde{s})^{-1/2} K_{l+1/2}(R\tilde{s})} \right) = \tilde{s} + \frac{1}{R} + \frac{1}{R^2} \hat{S}_l(R\tilde{s}), \quad (2.16)$$

where, for $l \neq 0$,

$$\hat{S}_l(z) = \frac{P_l(z)}{Q_l(z)}, \quad (2.17)$$

$$P_l(z) = \sum_{k=0}^{l-1} \frac{(2l-k)!}{k!(l-k-1)!} (2z)^k, \quad Q_l(z) = \sum_{k=0}^l \frac{(2l-k)!}{k!(l-k)!} (2z)^k,$$

and $S_0 = 0$. Returning to the time domain and denoting by \mathcal{H} the spherical harmonic transformation, we find

$$\frac{\partial u}{\partial \rho} + \frac{1}{c} \frac{\partial u}{\partial t} + \frac{1}{R} u + \frac{1}{R^2} \mathcal{H}^{-1} (S_l(ct/R) * (\mathcal{H}u)_l) = 0. \quad (2.18)$$

The rationality of \hat{S}_l implies that the temporal convolution in (2.18) can be localized, that is, its equivalent to the solution of a differential equation, albeit of order l . The localizability of the exact boundary condition was first noted and used by Sofronov (1993) and Grote and Keller (1995, 1996). We also have the following beautiful continued fraction representation for \hat{S}_l , which will play a role in efficient implementations of the exact condition:

$$\hat{S}_l(z) = \frac{l(l+1)}{2} \frac{1}{z+1 + \frac{l(l+1)-1.2}{4(z+2 + \frac{l(l+1)-2.3}{4(z+3+\dots)})}}. \quad (2.19)$$

It is also possible to derive analogous expressions for sphere-to-sphere extension operators. As mentioned earlier, these can be used in lieu of boundary conditions. The properties of localizability and ease of approximation which (2.18) possesses remain valid for the extension operators. In fact it is the extension formulation that is implemented in Sofronov (1999).

The construction of exact conditions on a spherical boundary is directly generalizable to conical domains. Precisely, we suppose Ξ may be described in spherical coordinates by

$$\Xi = \{(\rho, \theta, \phi) \in (R, \infty) \times \Theta\},$$

and that appropriate boundary conditions are imposed on $\partial\Theta$. Then we may separate variables as before except that we must expand in terms of the eigenfunctions of the Beltrami operator on Θ and, in (2.14), we must replace $-l(l+1)$ by the eigenvalues $-\kappa_l^2$. Then the transform of the exact boundary condition is as in (2.16) except that the index of the modified Bessel functions is

$$\nu = \sqrt{\kappa_l^2 + 1/4}.$$

Of course, for these indices, the exact condition is no longer a rational function of s , so that the operators are not equivalent to local operators in time. However, as we shall see later, this does not preclude their effective implementation.

Cylindrical boundary

We now take Γ to be the infinite cylinder described in standard cylindrical coordinates, (r, θ, z) , by $r = R$. Note that, just as in the case of a planar boundary, we may restrict z to a finite interval with the addition of appropriate boundary conditions and may also replace $\partial^2/\partial z^2$ by a more general

Sturm–Liouville operator. In the formulas that follow, this would simply require replacing Fourier transforms in z by Fourier series.

Thus, with k denoting the Fourier dual variable to z and l indexing the Fourier series in θ , we derive the ordinary differential equation

$$\frac{\partial^2 \hat{u}_l}{\partial r^2} + \frac{1}{r} \frac{\partial \hat{u}_l}{\partial r} - \left(\tilde{s}^2 + k^2 + \frac{l^2}{r^2} \right) \hat{u}_l = 0 \quad (2.20)$$

in the tail, with bounded solutions for $\text{Re } s > 0$ given by

$$\hat{u}_l = A_l(\tilde{s}, k) K_l(r\sqrt{\tilde{s}^2 + k^2}).$$

Here, again, K_l denotes the modified Bessel function of the third kind (Abramowitz and Stegun 1972, Ch. 9).

Using the well-known asymptotic expansions of K_l for large argument, found, for example, in the previously noted reference,

$$K_l(z) \sim \sqrt{\frac{\pi}{2z}} e^{-z},$$

we may again express the temporal part of the boundary condition as the sum of a local operator and convolution with a function. Precisely:

$$\begin{aligned} \hat{\mathcal{D}}_l &= -\sqrt{\tilde{s}^2 + k^2} \frac{K'_l(R\sqrt{\tilde{s}^2 + k^2})}{K_l(R\sqrt{\tilde{s}^2 + k^2})} \\ &= \tilde{s} + \frac{1}{2R} + (\sqrt{\tilde{s}^2 + k^2} - \tilde{s}) + \frac{1}{R^2} \hat{C}_l(R\sqrt{\tilde{s}^2 + k^2}), \\ \hat{C}_l(z) &= -z \left(\frac{K'_l(z)}{K_l(z)} + 1 + \frac{1}{2z} \right). \end{aligned} \quad (2.21)$$

In the time domain we have

$$\begin{aligned} \frac{\partial u}{\partial r} + \frac{1}{c} \frac{\partial u}{\partial t} + \frac{1}{2R} u + \mathcal{F}_z^{-1}(\mathcal{T}(\mathcal{F}_z u)) &= 0, \\ \mathcal{T} \bar{u} &= \left(ck^2 K(c|k|t) * \bar{u} + \frac{1}{R^2} \mathcal{F}_\theta^{-1}(G_l(ct, R, k) * (\mathcal{F}_\theta \bar{u})) \right), \end{aligned} \quad (2.22)$$

where $\mathcal{F}_{\theta, z}$ represents Fourier transformation in θ and z , respectively, and

$$G_l = \mathcal{L}^{-1}(\hat{C}_l(R\sqrt{\tilde{s}^2 + k^2})).$$

This result can be extended to domains where θ is restricted to a subinterval of $(\theta_0, \theta_1) \in (0, 2\pi)$ and additional boundary conditions are imposed. Then we need only change the index of the Bessel functions in (2.21) from l to κ_l where $-\kappa_l^2$ is the l th eigenvalue of $\partial^2/\partial\theta^2$.

We note that, in contrast with the spherical case, condition (2.22) cannot be exactly localized in time. However, as previously mentioned, the operators in all three cases may be very accurately and efficiently approximated

using essentially the same techniques. In particular, it is possible to express \hat{C}_l as the sum of a rational function and a function defined as an integral. Convergent approximations are derived in Sofronov (1999) by discretizing the integral. Similarly, the transform of the planar kernel may be expressed in integral form, and convergent approximations are derived in Hagstrom (1996) by discretization. In subsequent sections we will outline how these representations can be combined with multipole expansions to develop uniform approximations as in Alpert, Greengard and Hagstrom (1999b).

The dispersive wave equation

The dispersive wave equation is given by

$$\frac{1}{c^2} \frac{\partial^2 u}{\partial t^2} = \nabla^2 u - u. \quad (2.23)$$

Exact boundary conditions for (2.23) have precisely the same form as those for the wave equation, except that eigenvalues used in the definition of the nonlocal operators are shifted by one. Therefore we have, on a planar boundary, from (2.12):

$$\frac{\partial u}{\partial x} + \frac{1}{c} \frac{\partial u}{\partial t} + \mathcal{F}^{-1} \left(c(|k|^2 + 1)K(ct\sqrt{|k|^2 + 1}) * (\mathcal{F}u) \right) = 0.$$

On a sphere, using (2.18), we have

$$\frac{\partial u}{\partial \rho} + \frac{1}{c} \frac{\partial u}{\partial t} + \frac{1}{R} u + \frac{1}{R^2} \mathcal{H}^{-1} \left(\tilde{S}_l(ct/R) * (\mathcal{H}u)_l \right) = 0,$$

where

$$\tilde{S}_l = -R^2 \left(\frac{((R\tilde{s})^{-1/2} K_\nu(R\tilde{s}))'}{(R\tilde{s})^{-1/2} K_\nu(R\tilde{s})} + \tilde{s} + \frac{1}{R} \right),$$

and

$$\nu^2 = l(l+1) + \frac{5}{4}.$$

Note that this condition is not temporally localizable.

Finally, on a cylindrical boundary, we adapt (2.22):

$$\begin{aligned} \frac{\partial u}{\partial r} + \frac{1}{c} \frac{\partial u}{\partial t} + \frac{1}{2R} u + \mathcal{F}_z^{-1}(\tilde{T}(\mathcal{F}_z u)) &= 0, \\ \tilde{T}\bar{u} &= \left(c\gamma^2 K(c\gamma t) * \bar{u} + \frac{1}{R^2} \mathcal{F}_\theta^{-1}(\tilde{G}_l(ct, R, k) * (\mathcal{F}_\theta \bar{u})) \right), \end{aligned}$$

where

$$\gamma = \sqrt{|k|^2 + 1}, \quad \tilde{G}_l = \mathcal{L}^{-1}(\hat{C}_l(R\sqrt{\tilde{s}^2 + \gamma^2})),$$

and C_l is given by (2.21).

2.2. Generalizations to hyperbolic systems

Consider now a general first-order hyperbolic system with artificial boundary Γ given by the hyperplane $x = 0$, denoting as above the tangential variables by y . The equation in the tail takes the form

$$\frac{\partial u}{\partial t} = A_0 \frac{\partial u}{\partial x} + \sum_j B_j \frac{\partial u}{\partial y_j}, \tag{2.24}$$

where $u \in \mathbb{R}^q$, $A_0, B_j \in \mathbb{R}^{q \times q}$. We assume strong hyperbolicity. (See Kreiss and Lorenz (1989).) This implies, among other things, that the eigenvalues of

$$P = i \left(k_0 A_0 + \sum_j k_j B_j \right)$$

are purely imaginary for real k_j . To simplify the algebra, we also assume that the artificial boundary is noncharacteristic: that is, A_0 is invertible. Solving for $\partial u / \partial x$ and carrying out our usual Fourier–Laplace transformation in y and t we find:

$$\frac{\partial \hat{u}}{\partial x} = M \hat{u}, \quad M = A_0^{-1} \left(sI - \sum_j ik_j B_j \right). \tag{2.25}$$

By our assumption of hyperbolicity, for $\text{Re } s > 0$ no eigenvalue of M can lie on the imaginary axis, since that would imply a nonimaginary eigenvalue of P . Therefore, for $\text{Re } s > 0$ we may define two distinct invariant subspaces of M : the first, of dimension q_+ , is associated with eigenvalues with positive real part and the second, \hat{A} , of dimension $q_- = q - q_+$, is associated with eigenvalues with negative real part. Let $\hat{Q}_+^*(s, k)$ be a $q_+ \times q$ matrix of full rank all of whose rows are orthogonal to \hat{A} . Then an exact boundary condition at $x = 0$ is given, in the transform variables, by

$$\hat{Q}_+^* \hat{u} = 0.$$

Fixing k and letting s be large, standard results in matrix perturbation theory (Kato (1976, Ch. 2)) imply that we may rewrite this as

$$Q_{+,0}^* \hat{u} + \hat{Q}_+^*(s, k) \hat{u} = 0, \tag{2.26}$$

where the constant matrix $Q_{+,0}$ is determined by the invariant subspaces of A_0 , and hence may be taken so that $Q_{+,0}^* u$ defines the usual normal characteristic variables, and

$$\hat{Q}_+^* = O(|s|^{-1}), \quad s \rightarrow \infty.$$

Therefore the elements of \hat{Q}_+^* are the transforms of bounded functions and the temporal transform may be inverted to reveal a convolutional form:

$$Q_{+,0}^* u + \mathcal{F}^{-1} \left(\hat{Q}_+^* (\mathcal{F}u) \right) = 0. \quad (2.27)$$

The exact boundary condition at more general boundaries might be developed in the following way. At each point on the artificial boundary identify normal incoming and outgoing characteristics for the interior domain, Υ . For the tail, Ξ , the roles of these variables are reversed: outgoing for Υ is incoming for Ξ and vice versa. We parametrize solutions in the tail by their incoming data, thereby expressing the outgoing characteristic variables, from the perspective of Ξ , in terms of the incoming characteristic variables. From the perspective of the computational domain, Υ , we express incoming variables in terms of outgoing variables as expected. This construction is complicated by the fact that the number of incoming and outgoing characteristics will generally be different on different parts of the boundary, and we have not yet carried it out in any generality. An example where this difficulty occurs, namely the subsonic compressible Euler equations, is discussed below.

Systems equivalent to the wave equation: electromagnetism

Many hyperbolic systems of physical interest are isotropic. This, in addition to the requirement of homogeneity, forces them to be, in some sense, equivalent to systems of wave equations. Then, our formulations of exact boundary conditions for the wave equation can generally be translated into exact boundary conditions for the equivalent systems. A prime example of this is provided by the equations of electromagnetism. Of course, one can write these equations directly as a system of four wave equations for the vector and scalar potentials. (See, for instance, Schwartz (1987, Ch. 3).) Using the more conventional field variables, E and B , and assuming in Ξ an absence of charges or currents, we have Maxwell's system:

$$\frac{\partial E}{\partial t} - c \nabla \times B = 0, \quad (2.28)$$

$$\frac{\partial B}{\partial t} + c \nabla \times E = 0, \quad (2.29)$$

where c is the speed of light. In addition we have

$$\nabla \cdot E = \nabla \cdot B = 0. \quad (2.30)$$

(Of course E and B are uniquely determined by (2.28)–(2.29) and the initial and boundary conditions. However, it is easily seen that (2.30) is preserved under the time evolution.)

We begin with the simplest case of a planar boundary. Writing the system in the form (2.24) we note that the coefficient matrix corresponding to x -differentiation is singular, so that the boundary is characteristic. Applying Fourier transformation in the tangential variables and Laplace transformation in time leads to a differential-algebraic system where the algebraic equations are given by

$$\begin{aligned}\tilde{s}\hat{E}_1 &= ik_2\hat{B}_3 - ik_3\hat{B}_2, \\ \tilde{s}\hat{B}_1 &= -ik_2\hat{E}_3 + ik_3\hat{E}_2.\end{aligned}$$

Here $\tilde{s} = s/c$ and the subscript 1 denotes a field component in the x direction. Using the algebraic equations to eliminate \hat{E}_1 and \hat{B}_1 yields a system of four equations for $(\hat{E}_2, \hat{E}_3, \hat{B}_2, \hat{B}_3)^T$ in the form (2.25) where

$$M = \begin{pmatrix} 0 & 0 & \frac{k_2k_3}{\tilde{s}} & -\frac{(\tilde{s}^2+k_2^2)}{\tilde{s}} \\ 0 & 0 & \frac{(\tilde{s}^2+k_3^2)}{\tilde{s}} & -\frac{k_2k_3}{\tilde{s}} \\ -\frac{k_2k_3}{\tilde{s}} & \frac{(\tilde{s}^2+k_2^2)}{\tilde{s}} & 0 & 0 \\ -\frac{(\tilde{s}^2+k_3^2)}{\tilde{s}} & \frac{k_2k_3}{\tilde{s}} & 0 & 0 \end{pmatrix}.$$

The eigenvalues of M are given by

$$\lambda_{\pm} = \pm\sqrt{\tilde{s}^2 + k_2^2 + k_3^2},$$

where the branch is chosen as in our discussion of the wave equation. Exact boundary conditions may be determined by computing left eigenvectors corresponding to λ_+ . As this eigenspace is two dimensional, we may choose two independent eigenvectors which in turn will generate two boundary conditions. Note that the only nonlocal operator that can arise is expressed in terms of λ_+ , and hence will be the same as encountered in the case of the wave equation. One reasonable choice, which leads to symmetric formulae, is

$$\begin{aligned}&(\tilde{s}(\lambda_+ + \tilde{s}) + k_3^2, -k_2k_3, k_2k_3, -\tilde{s}(\lambda_+ + \tilde{s}) - k_2^2), \\ &(-k_2k_3, \tilde{s}(\lambda_+ + \tilde{s}) + k_2^2, \tilde{s}(\lambda_+ + \tilde{s}) + k_3^2, -k_2k_3).\end{aligned}$$

After some algebra, and the reintroduction of E_1 and B_1 to further simplify the results, we finally obtain

$$\frac{2}{c} \frac{\partial}{\partial t} (E_2 - B_3) + \mathcal{R} (E_2 - B_3) + \frac{\partial E_1}{\partial y} - \frac{\partial B_1}{\partial z} = 0, \quad (2.31)$$

$$\frac{2}{c} \frac{\partial}{\partial t} (E_3 + B_2) + \mathcal{R} (E_3 + B_2) + \frac{\partial E_1}{\partial z} + \frac{\partial B_1}{\partial y} = 0, \quad (2.32)$$

where \mathcal{R} is the nonlocal operator appearing in (2.12):

$$\mathcal{R}w = \mathcal{F}^{-1} \left(c|k|^2 K(c|k|t) * (\mathcal{F}w) \right).$$

Note that, by taking appropriate linear combinations, many other forms could be obtained.

Similarly, exact conditions at spherical and cylindrical boundaries for the Maxwell system involve the nonlocal operators appearing in (2.18) and (2.22), the exact conditions for the wave equation. Again, a number of formulations are possible, as each field component solves the wave equation individually and hence satisfies that equation's exact boundary condition. Of course, not all such formulations are well-posed. Below we outline a direct derivation in the spherical case which involves the application of the nonlocal operator to a minimal number of quantities and is hence somewhat less expensive to implement. For an alternative form see Grote and Keller (1999), where the authors adapt their derivation of local exact conditions for the wave equation.

We begin by performing a Laplace transformation in time and expanding E and B in the orthogonal basis of vector spherical harmonics (Newton 1966, Ch. 2):

$$\begin{aligned} \hat{E} &= \sum_l \left(\hat{E}_{0,l} Y_l^{(0)} + \hat{E}_{e,l} Y_l^{(e)} + \hat{E}_{m,l} Y_l^{(m)} \right), \\ \hat{B} &= \sum_l \left(\hat{B}_{0,l} Y_l^{(0)} + \hat{B}_{e,l} Y_l^{(e)} + \hat{B}_{m,l} Y_l^{(m)} \right), \end{aligned}$$

where

$$Y_l^{(0)} = Y_l e_\rho, \quad Y_l^{(e)} = \frac{\partial Y_l}{\partial \theta} e_\theta + \frac{1}{\sin \theta} \frac{\partial Y_l}{\partial \phi} e_\phi, \quad Y_l^{(m)} = -\frac{1}{\sin \theta} \frac{\partial Y_l}{\partial \phi} e_\theta + \frac{\partial Y_l}{\partial \theta} e_\phi, \quad (2.33)$$

and e_ρ , e_θ and e_ϕ are the standard unit basis vectors in the spherical coordinate system. As in the case of a planar boundary, Maxwell's equations now lead to a differential-algebraic system in ρ for the expansion coefficients. The algebraic equations may be used to eliminate the coefficients associated with the radial harmonics, $Y_l^{(0)}$:

$$\begin{aligned} \tilde{s} \hat{E}_{0,l} &= -\frac{l(l+1)}{\rho} \hat{B}_{m,l}, \\ \tilde{s} \hat{B}_{0,l} &= \frac{l(l+1)}{\rho} \hat{E}_{m,l}. \end{aligned}$$

We then have the following first-order system for the remaining variables:

$$\left(\frac{\partial}{\partial \rho} + \frac{1}{\rho}\right) \begin{pmatrix} \hat{E}_{e,l} \\ \hat{E}_{m,l} \\ \hat{B}_{e,l} \\ \hat{B}_{m,l} \end{pmatrix} = \tilde{s} \begin{pmatrix} 0 & 0 & 0 & -1 - \frac{l(l+1)}{\rho^2 \tilde{s}^2} \\ 0 & 0 & 1 & 0 \\ 0 & 1 + \frac{l(l+1)}{\rho^2 \tilde{s}^2} & 0 & 0 \\ -1 & 0 & 0 & 0 \end{pmatrix} \begin{pmatrix} \hat{E}_{e,l} \\ \hat{E}_{m,l} \\ \hat{B}_{e,l} \\ \hat{B}_{m,l} \end{pmatrix}.$$

Bounded solutions are given by

$$\alpha_l \begin{pmatrix} k'_l(\rho \tilde{s}) + \frac{k_l(\rho \tilde{s})}{\rho \tilde{s}} \\ 0 \\ 0 \\ -k_l(\rho \tilde{s}) \end{pmatrix} + \beta_l \begin{pmatrix} 0 \\ k_l(\rho \tilde{s}) \\ k'_l(\rho \tilde{s}) + \frac{k_l(\rho \tilde{s})}{\rho \tilde{s}} \\ 0 \end{pmatrix},$$

where k_l is the modified spherical Bessel function of the third kind (2.15). In terms of the expansion coefficients this may be written as

$$\begin{aligned} \tilde{s} (\hat{E}_{l,m} + \hat{B}_{l,e}) + \frac{1}{\rho^2} \hat{S}_l(\rho \tilde{s}) \hat{E}_{l,m} &= 0, \\ \tilde{s} (\hat{E}_{l,e} - \hat{B}_{l,m}) - \frac{1}{\rho^2} \hat{S}_l(\rho \tilde{s}) \hat{B}_{l,m} &= 0, \end{aligned}$$

where \hat{S}_l is as in (2.16).

Finally, we note that if we define $\tilde{B} = e_\rho \times B = -B_\phi e_\theta + B_\theta e_\phi$ then

$$\hat{B}_{l,e} = \hat{B}_{l,m}, \quad -\hat{B}_{l,m} = \hat{B}_{l,e}.$$

Therefore, letting $\rho = R$ be the boundary location and inverting the transforms we reach our final form:

$$\begin{aligned} \frac{1}{c} \frac{\partial}{\partial t} \begin{pmatrix} E_\theta - B_\phi \\ E_\phi + B_\theta \end{pmatrix} + \tag{2.34} \\ \frac{1}{R^2} \sum_l \left(Y_l^{(m)}(S_l(ct/R) * E_{l,m}) - Y_l^{(e)}(S_l(ct/R) * B_{l,e}) \right) &= 0. \end{aligned}$$

Not surprisingly, it is also possible to formulate the exact boundary condition on a cylinder using the nonlocal operator in (2.22), but we will present the details elsewhere.

Systems equivalent to the wave equation: elasticity

The equations of linear elasticity in an isotropic medium are typically formulated in terms of a 3-vector, u , describing the displacements (Eringen and Şuhubi 1975, Ch. 5). They are given by Navier’s equations:

$$\frac{\partial^2 u}{\partial t^2} = (c_t^2 - c_l^2) \nabla(\nabla \cdot u) + c_t^2 \nabla^2 u, \tag{2.35}$$

where c_l and c_t are the irrotational and equivoluminal sound speeds, respectively. Unlike the case of Maxwell's equations, each component of u does not satisfy the scalar wave equation. However, a Helmholtz decomposition of u produces a vector and a scalar wave equation, one with each wave speed. We shall proceed directly, deriving expressions for the exact boundary condition at planar and spherical boundaries.

The direct approach to deriving exact boundary conditions on the plane $x = 0$ is to reduce the problem to a first-order system in x , carry out a Fourier–Laplace transform in (y, t) , and compute the requisite projection operators into the admissible subspace, $\hat{\mathcal{A}}$, as described above. However, as this is a second-order system, we will jump ahead and look for the Dirichlet-to-Neumann map. Seeking solutions of the form

$$\hat{u} = e^{\lambda x + st + ik \cdot y} v$$

leads to the algebraic system

$$\left((c_t^2(\lambda^2 - |k|^2) - s^2)I + (c_l^2 - c_t^2)ww^T \right) v = 0, \quad w = \begin{pmatrix} \lambda \\ ik \end{pmatrix}. \quad (2.36)$$

There are three independent bounded solutions of this system. Two correspond to the equivoluminal modes

$$\lambda_t = -\sqrt{(s^2/c_t^2) + |k|^2}, \quad v_1 = \begin{pmatrix} |k|^2 \\ \lambda_t \\ ik \end{pmatrix}, \quad v_2 = \begin{pmatrix} 0 \\ iq \end{pmatrix},$$

where the 2-vector q is orthogonal to k ,

$$q = \begin{pmatrix} -k_2 \\ k_1 \end{pmatrix}.$$

The third corresponds to the irrotational mode

$$\lambda_l = -\sqrt{(s^2/c_l^2) + |k|^2}, \quad v_3 = \begin{pmatrix} \lambda_l \\ ik \end{pmatrix}.$$

Setting V to be the matrix whose columns are v_i , we have at $x = 0$, for some 3-vector \hat{c} ,

$$\hat{u} = V\hat{c}, \quad \frac{\partial \hat{u}}{\partial x} = V\Lambda\hat{c}, \quad \Lambda = \text{diag}(\lambda_t, \lambda_t, \lambda_l).$$

Therefore

$$\hat{\mathcal{D}} = -V\Lambda V^{-1},$$

where, after some algebra, we find

$$\hat{\mathcal{D}} = \begin{pmatrix} -\lambda_l + \gamma_d & \frac{(c_l - c_t)}{c_l}(1 + c_t\gamma_s)ik^T \\ \frac{(c_l - c_t)}{c_t}(1 - c_l\gamma_s)ik & (-\lambda_t - \gamma_d)\frac{kk^T}{|k|^2} - \lambda_t\frac{qq^T}{|k|^2} \end{pmatrix},$$

and

$$\gamma_d = \frac{(c_l^2 - c_t^2)|k|^2}{c_l^2 \lambda_l + c_t^2 \lambda_t}, \quad \gamma_s = \frac{(c_l^2 - c_t^2)|k|^2}{(c_l^2 \lambda_l + c_t^2 \lambda_t)(c_l \lambda_l + c_t \lambda_t)}.$$

Returning to the time domain and using the fact that $(kk^T + qq^T) = |k|^2 I$, we find

$$\frac{\partial u}{\partial x} + \Sigma \frac{\partial u}{\partial t} + Cu + \mathcal{F}^{-1} (E * (\mathcal{F}u)) = 0, \quad (2.37)$$

where

$$\Sigma = \text{diag}(1/c_l, 1/c_t, 1/c_t), \quad C = \begin{pmatrix} 0 & \frac{(c_l - c_t)}{c_l} ik^T \\ \frac{(c_l - c_t)}{c_t} ik & 0 \end{pmatrix}.$$

The transform of the nonlocal operator of E is given by

$$\hat{E} = \begin{pmatrix} -\lambda_l - \frac{s}{c_l} + \gamma_d & \frac{(c_l - c_t)}{c_l} c_t \gamma_s ik^T \\ -\frac{(c_l - c_t)}{c_t} c_l \gamma_s ik & (-\lambda_t - \frac{s}{c_t}) I - \gamma_d \frac{kk^T}{|k|^2} \end{pmatrix}.$$

We see that it involves both the kernel K , through the terms $\lambda_t + s/c_t$ and $\lambda_l + s/c_l$, as well as some new kernels whose transforms are γ_d and γ_s .

As for Maxwell's equations, exact conditions at a spherical boundary are most easily obtained by expanding the solution, u , in terms of vector spherical harmonics (2.33). Denoting the transformed expansion coefficients by $\hat{u}_{l,0}$, $\hat{u}_{l,e}$ and $\hat{u}_{l,m}$, we derive, after some algebra, the following equations where prime denotes differentiation with respect to ρ :

$$s^2 \hat{u}_{l,0} = c_t^2 l(l+1) \left(\frac{\hat{u}'_{l,e}}{\rho} + \frac{\hat{u}_{l,e}}{\rho^2} - \frac{\hat{u}_{l,0}}{\rho^2} \right) + c_t^2 \left(\hat{u}''_{l,0} + \frac{2}{\rho} \hat{u}'_{l,0} - \frac{2}{\rho^2} \hat{u}_{l,0} - l(l+1) \left(\frac{\hat{u}'_{l,e}}{\rho} - \frac{\hat{u}_{l,e}}{\rho^2} \right) \right),$$

$$s^2 \hat{u}_{l,e} = c_t^2 l(l+1) \left(\hat{u}''_{l,e} + \frac{2}{\rho} \hat{u}'_{l,e} - \frac{\hat{u}'_{l,0}}{\rho} \right) + c_t^2 \left(\frac{\hat{u}'_{l,0}}{\rho} + \frac{2}{\rho^2} \hat{u}_{l,0} - l(l+1) \frac{\hat{u}_{l,e}}{\rho^2} \right),$$

$$s^2 \hat{u}_{l,m} = c_t^2 \left(\hat{u}''_{l,m} + \frac{2}{\rho} \hat{u}'_{l,m} - \frac{l(l+1)}{\rho^2} \hat{u}_{l,m} \right).$$

Bounded solutions of this system, which may also be directly derived via a Helmholtz decomposition as in Eringen and Şuhubi (1975, Ch. 8) are

described by

$$\begin{pmatrix} \hat{u}_{l,0} \\ \hat{u}_{l,e} \\ \hat{u}_{l,m} \end{pmatrix} = \begin{pmatrix} \frac{s}{c_t} k_l'(\rho s/c_l) & \frac{l(l+1)}{\rho} k_l(\rho s/c_t) & 0 \\ \frac{k_l(\rho s/c_l)}{\rho} & \frac{1}{\rho} \frac{\partial}{\partial \rho} (\rho k_l(\rho s/c_t)) & 0 \\ 0 & 0 & k_l(\rho s/c_t) \end{pmatrix} \begin{pmatrix} \alpha_l \\ \beta_l \\ \gamma_l \end{pmatrix},$$

where k_l is again given by (2.15). Denoting by B the matrix above, the Dirichlet-to-Neumann map is defined by the matrix

$$\hat{D}_l = -\frac{\partial B}{\partial \rho} B^{-1}.$$

It is clear from the structure of the matrix B that the entries of \hat{D}_l will be rational functions of s . Hence \hat{D}_l corresponds to a localizable operator in time. Separating out the local part of the operator, we reach the form

$$\hat{D}_l = s\Sigma + \frac{1}{R} \begin{pmatrix} 1 & l(l+1) \frac{c_t - c_l}{c_l} & 0 \\ \frac{c_l - c_t}{c_t} & 1 & 0 \\ 0 & 0 & 1 \end{pmatrix} + \frac{1}{R^2} \begin{pmatrix} \hat{P}_l & 0 \\ 0^T & \hat{S}_l(Rs/c_t) \end{pmatrix}.$$

The elements of the 2×2 matrix \hat{P}_l are rational functions of s of degree no more than $(2l+3, 2l+4)$. We have not yet studied them in any detail. Writing

$$u = \begin{pmatrix} u_\rho \\ u_\theta \\ u_\phi \end{pmatrix},$$

using the identities

$$\begin{aligned} \hat{u}_{\text{norm}} &= \sum_l \hat{u}_{l,0} Y_l^{(0)}, & \hat{u}_{\text{tan}} &= \sum_l (\hat{u}_{l,e} Y_l^{(e)} + \hat{u}_{l,m} Y_l^{(m)}), \\ \nabla \cdot \hat{u}_{\text{tan}} &= -\sum_l \frac{l(l+1)}{\rho} \hat{u}_{l,e}, & e_\rho \times (\nabla \times \hat{u}_{\text{norm}}) &= \sum_l \frac{1}{\rho} \hat{u}_{l,0} Y_l^{(e)}, \end{aligned}$$

and inverting the transforms, we find

$$\begin{aligned} \frac{\partial u}{\partial \rho} + \Sigma \frac{\partial u}{\partial t} + \frac{1}{R} u + \frac{c_l - c_t}{c_l} e_\rho (\nabla \cdot u_{\text{tan}}) + \frac{c_l - c_t}{c_t} e_\rho \times (\nabla \times u_{\text{norm}}) \\ + \frac{1}{R^2} \mathcal{H}^{-1} \left(\begin{pmatrix} P_l^* & 0 \\ 0^T & S_l^* \end{pmatrix} (\mathcal{H}u) \right) = 0. \end{aligned}$$

A direct derivation of an exact local form, based on the Helmholtz decomposition and their approach to the wave equation, was first given by Grote and Keller (1998).

Linearized gas dynamics: a problem with anisotropy

In all the examples above which we have studied in detail, the system has been isotropic. A consequence of this is that the number of boundary conditions required is independent of the location on the boundary. We now consider an important system for which this is not the case.

The linearized, subsonic Euler system for a polytropic gas in three space dimensions is given by

$$\frac{\partial q}{\partial t} + \sum_{j=1}^3 A_j \frac{\partial q}{\partial x_j} = 0,$$

where

$$q = \begin{pmatrix} \rho \\ u_1 \\ u_2 \\ u_3 \\ T \end{pmatrix}, \quad A_j = U_j I + \begin{pmatrix} 1 \\ 0 \\ 0 \\ 0 \\ \gamma - 1 \end{pmatrix} e_{j+1}^T + e_{j+1} \begin{pmatrix} \gamma^{-1} \\ 0 \\ 0 \\ 0 \\ \gamma^{-1} \end{pmatrix}^T,$$

where e_{j+1} is the $(j + 1)$ th unit 5-vector, ρ is the density perturbation, u_j the velocity perturbations, and T the temperature perturbation. Finally, we assume

$$U_1 \neq 0, \quad \sum_j U_j^2 < 1.$$

Applying a Fourier–Laplace transformation with dual variables (k_2, k_3, s) , and solving for x -derivatives, we obtain a system in the form (2.25) with M given by

$$\begin{pmatrix} \frac{\bar{s}(1-\gamma(1-U_1^2))}{\gamma U_1(1-U_1^2)} & -\frac{\bar{s}}{1-U_1^2} & \frac{ik_2 U_1}{1-U_1^2} & \frac{ik_3 U_1}{1-U_1^2} & \frac{\bar{s}}{\gamma U_1(1-U_1^2)} \\ -\frac{\bar{s}}{\gamma(1-U_1^2)} & \frac{\bar{s}U_1}{1-U_1^2} & -\frac{ik_2}{1-U_1^2} & -\frac{ik_3}{1-U_1^2} & -\frac{\bar{s}}{\gamma(1-U_1^2)} \\ -\frac{ik_2}{\gamma U_1} & 0 & -\frac{\bar{s}}{U_1} & 0 & -\frac{ik_2}{\gamma U_1} \\ -\frac{ik_3}{\gamma U_1} & 0 & 0 & -\frac{\bar{s}}{U_1} & -\frac{ik_3}{\gamma U_1} \\ \frac{\bar{s}(\gamma-1)}{\gamma U_1(1-U_1^2)} & -\frac{\bar{s}(\gamma-1)}{1-U_1^2} & \frac{ik_2(\gamma-1)U_1}{1-U_1^2} & \frac{ik_3(\gamma-1)U_1}{1-U_1^2} & \frac{\bar{s}(\gamma U_1^2-1)}{\gamma U_1(1-U_1^2)} \end{pmatrix},$$

where

$$\bar{s} = s + ik_2 U_2 + ik_3 U_3.$$

The eigenvalues of M are given by

$$\lambda_{\pm} = \frac{\bar{s}U_1 \pm \sqrt{\bar{s}^2 + (1 - U_1^2)|k|^2}}{1 - U_1^2},$$

and a triple eigenvalue

$$\lambda_0 = -\frac{\tilde{s}}{U_1}.$$

Setting

$$\mu = \sqrt{\tilde{s}^2 + (1 - U_1^2)|k|^2},$$

five left eigenvectors are given by

$$\begin{aligned} l_+ &= \begin{pmatrix} \frac{\mu}{\gamma} & -\tilde{s} & ik_2U_1 & ik_3U_1 & \frac{\mu}{\gamma} \end{pmatrix}, \\ l_- &= \begin{pmatrix} \frac{\mu}{\gamma} & \tilde{s} & -ik_2U_1 & -ik_3U_1 & \frac{\mu}{\gamma} \end{pmatrix}, \\ l_{0,1} &= (\gamma - 1 \quad 0 \quad 0 \quad 0 \quad -1), \\ l_{0,2} &= (ik_2 \quad ik_2U_1 \quad \tilde{s} \quad 0 \quad 0), \\ l_{0,3} &= (ik_3 \quad ik_3U_1 \quad 0 \quad \tilde{s} \quad 0). \end{aligned}$$

Note that the signs of the real parts of the eigenvalues, and the number with positive and negative real part, depends on the sign of U_1 . I will as usual assume that Υ lies to the left of $x = 0$, so that the outflow case corresponds to $U_1 > 0$ and the inflow case to $U_1 < 0$.

Outflow boundary. At outflow we require one boundary condition, corresponding to the single incoming characteristic or, equivalently, the single eigenvalue λ_+ with positive real part. The boundary condition is defined by l_+ . After inverting the transforms we find

$$\frac{D_{\tan}}{Dt}(p - u) + \tilde{\mathcal{R}}p + U_1 \left(\frac{\partial u_2}{\partial y} + \frac{\partial u_3}{\partial z} \right) = 0, \quad (2.38)$$

where we have introduced the pressure perturbation,

$$p = \gamma^{-1}(\rho + T),$$

and

$$\begin{aligned} \frac{D_{\tan} w}{Dt} &= \frac{\partial w}{\partial t} + U_2 \frac{\partial w}{\partial y} + U_3 \frac{\partial w}{\partial z}, \\ \tilde{\mathcal{R}}w &= \mathcal{F}^{-1} \left((1 - U_1^2)|k|^2 \tilde{K}(k, t) * (\mathcal{F}w) \right), \\ \tilde{K}(k, t) &= e^{-i(U_2 k_2 + U_3 k_3)t} K(\sqrt{1 - U_1^2}|k|t). \end{aligned}$$

Inflow boundary. At inflow, that is, if $U_1 < 0$, we require four boundary conditions as the triple eigenvalue λ_0 is now positive. It would be natural to simply append the three conditions defined by $l_{0,j}$ to the condition defined by l_+ . However, when $\tilde{s} = -|k|U_1 > 0$, $\lambda_+ = \lambda_0$ and l_+ is in the span of the $l_{0,j}$. Therefore, the straightforward construction leads to ill-posed problems. (See also Giles (1990).) This may be remedied by replacing l_+ with

an appropriate linear combination of the four conditions. One possibility, analogous to the one used in two-dimensional computations by Hagstrom and Goodrich (1998), is

$$\tilde{l} = \begin{pmatrix} \frac{\tilde{s}+\mu}{\gamma} & -(\tilde{s} + \mu) & ik_2(1 + U_1) & ik_3(1 + U_1) & \frac{\tilde{s}+\mu}{\gamma} \end{pmatrix}.$$

This leads to the system of four boundary conditions:

$$\frac{D_{\tan}}{Dt}(p - u_1) + \frac{1}{2}\tilde{\mathcal{R}}(p - u_1) + \frac{1 + U_1}{2} \left(\frac{\partial u_2}{\partial y} + \frac{\partial u_3}{\partial z} \right) = 0, \quad (2.39)$$

$$(\gamma - 1)\rho - T = 0, \quad (2.40)$$

$$\frac{D_{\tan}u_2}{Dt} + \frac{\partial \rho}{\partial y} + U_1 \frac{\partial u_1}{\partial y} = 0, \quad (2.41)$$

$$\frac{D_{\tan}u_3}{Dt} + \frac{\partial \rho}{\partial z} + U_1 \frac{\partial u_1}{\partial z} = 0. \quad (2.42)$$

The stability of these conditions and derived approximations will be shown by Goodrich and Hagstrom (1999). Note that (2.40) is simply the statement that the entropy perturbation is zero at inflow. Using it and the momentum equations we see that (2.41) and (2.42) are equivalent to setting to zero the tangential components of the vorticity at the boundary

$$\frac{\partial u_2}{\partial x} = \frac{\partial u_1}{\partial y}, \quad \frac{\partial u_3}{\partial x} = \frac{\partial u_1}{\partial z}.$$

The boundary condition for the acoustic modes is related to exact boundary conditions for the convective wave equation satisfied by the pressure, p . Precisely, it may be obtained from this exact condition and the use of the equations to eliminate the normal p derivative.

As mentioned earlier, we have no direct derivation of exact conditions for exterior problems with anisotropy. However, the interpretation above is suggestive of an *ad hoc* approach, which may work in this important case. In particular, the analogues of (2.40)–(2.41), namely the specification of zero entropy and tangential vorticity perturbations, are valid at inflow for any convex boundary. This leaves us with the problem of deriving exact conditions for the convective wave equation satisfied by the pressure perturbation, and then coupling it with the equations and boundary conditions to produce a well-posed problem. These latter problems to date are unsolved.

2.3. Equations of mixed order

Although the vast majority of work on radiation boundary conditions has been concentrated on the hyperbolic case, it is possible to apply the same general principles to construct exact boundary conditions for equations of different types. In this section we consider examples that involve partial

differential operators of first order in time but second order in the spatial variables. The major difference, in comparison with the hyperbolic case, is in the dependence of the symbol of the exact operator on the dual variable to time, s . (See Halpern and Rauch (1995) for a discussion of the appropriate symbol classes in the case of parabolic systems.) In particular, we cannot write the operator as the sum of a local operator and a temporal convolution with a bounded kernel, but rather write it as convolution composed with time differentiation. Our three examples will include the scalar advection–diffusion equation, the Schrödinger equation, and the incompressible Navier–Stokes equations. All three cases will be treated in three space dimensions at planar boundaries and all but the Navier–Stokes equations at spherical boundaries. As the reader is now experienced with the separation-of-variables techniques for deriving the boundary conditions, I will omit some of the details.

The advection–diffusion equation

Consider the scalar advection–diffusion equation

$$\frac{\partial u}{\partial t} + U \cdot \nabla u = \nu \nabla^2 u, \quad (2.43)$$

in the half, Ξ , defined by $x > 0$. After Fourier–Laplace transformation, we derive the following expression for bounded solutions:

$$\hat{u} = A(s, k)e^{-\lambda x}, \quad \lambda = \frac{s + iU_{\text{tan}} \cdot k + \nu|k|^2}{U_1/2 + \sqrt{\nu(s + iU_{\text{tan}} \cdot k + \nu|k|^2) + U_1^2/4}}, \quad (2.44)$$

with the exact boundary condition given by

$$\frac{\partial \hat{u}}{\partial x} + \lambda \hat{u} = 0.$$

Here we have written $U = (U_1, U_{\text{tan}})^T$ and chosen a branch of the square root with positive real part for $\text{Re } s > 0$. Note that we cannot write λ as the sum of a polynomial in s and the transform of a function. However, we can return to the time domain, finding:

$$\frac{\partial u}{\partial x} + \mathcal{F}^{-1}(W_+ * (\mathcal{F}(Nu))) = 0, \quad (2.45)$$

$$Nu = \frac{\partial u}{\partial t} + U_{\text{tan}} \cdot \nabla_y u - \nu \nabla_y^2 u,$$

$$W_+ = \frac{1}{\nu} e^{-\left(iU_{\text{tan}} \cdot k + \nu|k|^2 + \frac{U_1^2}{4\nu}\right)t} \left(\sqrt{\frac{\nu}{\pi t}} - \frac{U_1}{2} e^{\frac{U_1^2 t}{4\nu}} \text{Erfc} \left(\frac{U_1}{2} \sqrt{\frac{t}{\nu}} \right) \right).$$

(The formulas leading to W_+ may be found in Oberhettinger and Badii (1970).)

Similarly, we can treat the case of a spherical boundary. Clearly, without loss of generality, we may assume that the advection field, U , is in the x direction. Then we have

$$s\hat{u} + U_1 \frac{\partial \hat{u}}{\partial x} = \nu \nabla^2 \hat{u}.$$

Set

$$\hat{u} = e^{\frac{U_1 x}{2\nu}} \hat{v}.$$

Then, \hat{v} satisfies

$$\left(s + \frac{U_1^2}{4\nu} \right) \hat{v} = \nu \nabla^2 \hat{v}.$$

Therefore, repeating our analysis from the case of the wave equation, (2.16), we find

$$\begin{aligned} \frac{\partial \hat{u}}{\partial \rho} &= \frac{U_1}{2\nu} \sin \theta \cos \phi \hat{u} + e^{\frac{U_1 x}{2\nu}} \frac{\partial \hat{v}}{\partial \rho} \\ &= \frac{U_1}{2\nu} \sin \theta \cos \phi \hat{u} \\ &\quad - e^{\frac{U_1 x}{2\nu}} \sum_l \left(\frac{\sqrt{4\nu s + U_1^2}}{2\nu} + \frac{1}{R} + \frac{1}{R^2} \hat{S}_l \left(\frac{R}{2\nu} \sqrt{4\nu s + U_1^2} \right) \right) \hat{v}_l Y_l(\theta, \phi). \end{aligned}$$

Inverting the Laplace transform we reach our final form:

$$\begin{aligned} \frac{\partial u}{\partial \rho} - \frac{U_1}{2\nu} \sin \theta \cos \phi u + P * \left(\frac{\partial u}{\partial t} + \frac{U_1^2}{4\nu} u \right) + \frac{1}{R} u + \\ \frac{1}{R^2} e^{\frac{U_1 x}{2\nu}} \mathcal{H}^{-1} \left(\bar{S}_l * (\mathcal{H}(e^{-\frac{U_1 x}{2\nu}} u))_l \right) = 0, \quad (2.46) \end{aligned}$$

where

$$P(t) = (\pi \nu t)^{-1/2} e^{-\frac{U_1^2 t}{4\nu}}, \quad \bar{S}_l(R, t) = \mathcal{L}^{-1} \hat{S}_l(R \sqrt{4\nu s + U_1^2} / (2\nu)).$$

Due to the presence of the irrational function of s in the argument of \hat{S}_l , (2.46) cannot be directly expressed as a local operator. We note that the special case of the heat equation is recovered by setting $U = 0$. For the heat equation, however, fast methods for evaluating the solution operator are available (Greengard and Lin 1998), which may lead to more efficient methods of solution in most cases.

The Schrödinger equation

The Schrödinger equation is defined by

$$-i \frac{\partial u}{\partial t} = \nabla^2 u.$$

Clearly, representations of exact boundary conditions in transform space may be obtained from those above by setting $U = 0$, replacing s by $-is$ and choosing appropriate branches. For the case of a planar boundary, define $\sqrt{-is + |k|^2}$ so that, for $\text{Re } s > 0$,

$$\text{Re} \left(\sqrt{-is + |k|^2} \right) > 0. \quad (2.47)$$

Then, on the planar boundary $x = 0$ we have, in analogy with (2.45),

$$\begin{aligned} \frac{\partial u}{\partial x} + \mathcal{F}^{-1} \left(\tilde{W} * (\mathcal{F}(Tu)) \right) &= 0, \\ Tu = -i \frac{\partial u}{\partial t} - \nabla_y^2 u, \quad \tilde{W} &= e^{-i|k|^2 t + i\pi/4} (\pi t)^{-1/2}. \end{aligned}$$

On the spherical boundary, choosing $\sqrt{-is}$ according to (2.47), we adapt (2.46) and find

$$\frac{\partial u}{\partial \rho} + Q * \left(e^{-i\pi/4} \frac{\partial u}{\partial t} \right) + \frac{1}{R} u + \frac{1}{R^2} \mathcal{H}^{-1} \left(\tilde{S}_l * (\mathcal{H}u)_l \right) = 0,$$

where

$$Q(t) = (\pi t)^{-1/2}, \quad \tilde{S}_l(R, t) = \mathcal{L}^{-1} \hat{S}_l(R\sqrt{-is}).$$

The linearized incompressible Navier–Stokes equations

As our final example of an equation of mixed order, we consider the construction of exact boundary conditions at a planar boundary for the Navier–Stokes equations linearized about a uniform flow. Again we shall see that our general techniques apply, and that the temporally nonlocal operators that arise are the same which are needed in the case of the advection–diffusion equation. (For alternative constructions in each case see Halpern (1986), Halpern and Schatzman (1989).)

We thus consider

$$\nabla \cdot u = 0,$$

$$\frac{\partial u}{\partial t} + U \cdot u + \nabla p = \nu \nabla^2 u,$$

in the tail $\Xi \subset \mathbb{R}^3$ defined by $x > 0$. We make no restrictions on U_1 so that there may be either inflow or outflow at the boundary. Following our standard construction, we perform a Fourier–Laplace transformation and make the system first order in x . Here we use the divergence constraint to

eliminate $\partial u_1/\partial x$, leading to a system of six equations:

$$\frac{\partial w}{\partial x} = Mw, \quad w = \begin{pmatrix} \hat{p} \\ \hat{u}_1 \\ \hat{u}_2 \\ \hat{u}_3 \\ \nu \frac{\partial \hat{u}_2}{\partial x} \\ \nu \frac{\partial \hat{u}_3}{\partial x} \end{pmatrix},$$

$$M = \begin{pmatrix} 0 & -\tilde{s} & ik_2U_1 & ik_3U_1 & -ik_2 & -ik_3 \\ 0 & 0 & -ik_2 & -ik_3 & 0 & 0 \\ 0 & 0 & 0 & 0 & \nu^{-1} & 0 \\ 0 & 0 & 0 & 0 & 0 & \nu^{-1} \\ ik_2 & 0 & \tilde{s} & 0 & U_1\nu^{-1} & 0 \\ ik_3 & 0 & 0 & \tilde{s} & 0 & U_1\nu^{-1} \end{pmatrix},$$

where $\tilde{s} = s + iU_{\tan} \cdot k + \nu|k|^2$.

The eigenvalues of M are

$$\lambda_1 = |k|, \quad \lambda_{2,3} = \frac{U_1 + \gamma}{2\nu}, \quad \lambda_4 = -|k|, \quad \lambda_{5,6} = \frac{U_1 - \gamma}{2\nu},$$

with γ satisfying $\text{Re } \gamma > 0$ when $\text{Re } s > 0$ is defined by

$$\gamma = \sqrt{4\nu\tilde{s} + U_1^2}.$$

It is natural to define exact boundary conditions by the left eigenvectors associated with $\lambda_{1,2,3}$ which may be given by

$$\begin{aligned} q_1 &= |k|^{-1}(-|k|, \tilde{s}, -ik_2U_1, -ik_3U_1, ik_2, ik_3), \\ q_2 &= \frac{2}{U_1 + \gamma} \left(ik_2, -2\frac{ik_2\nu\tilde{s}}{U_1 + \gamma}, \tilde{s} - \nu k_2^2, -\nu k_2 k_3, \frac{U_1 + \gamma}{2\nu}, 0 \right), \\ q_3 &= \frac{2}{U_1 + \gamma} \left(ik_3, -2\frac{ik_3\nu\tilde{s}}{U_1 + \gamma}, -\nu k_2 k_3, \tilde{s} - \nu k_3^2, 0, \frac{U_1 + \gamma}{2\nu} \right). \end{aligned}$$

However, when $\tilde{s} = \nu|k|^2 - U_1|k|$, $\lambda_1 = \lambda_{2,3}$, and we find that q_1 is in the span of $q_{2,3}$. Therefore we replace it by a linear combination of the three eigenvectors which remains independent of $q_{2,3}$:

$$-\left(1, -\tilde{z}(1 + \nu|k|\hat{W}_+), ik_2\nu(1 + \tilde{z}W_-), ik_3\nu(1 + \tilde{z}W_-), 0, 0\right),$$

where $\tilde{z} = |k|^{-1}\tilde{s}$ and

$$\hat{W}_{\pm} = \frac{2\nu}{\pm U_1 + \gamma}.$$

Introducing the operators

$$H = \mathcal{F}^{-1}(|k|^{-1}\mathcal{F}u), \quad N = \left(\frac{\partial}{\partial t} + U_{\tan} \cdot \nabla - \nu \nabla_{\tan}^2 \right),$$

the kernels

$$W_{\pm} = e^{-(iU_{\tan} \cdot k + \nu|k|^2 + \frac{\nu_1^2}{4\nu})t} \left(\sqrt{\frac{\nu}{\pi t}} \mp \frac{U_1}{2} e^{\frac{\nu_1^2 t}{4\nu}} \operatorname{Erfc} \left(\pm \frac{U_1}{2} \sqrt{\frac{t}{\nu}} \right) \right),$$

which we recognize from our study of the advection–diffusion equation, and the temporally nonlocal operator $\mathcal{W}_{\pm}u = \mathcal{F}^{-1}(W_{\pm} * (\mathcal{F}u))$, the exact conditions in the time domain are expressed by

$$-p + \nu \frac{\partial u_1}{\partial x} + (H + \mathcal{W}_+)Nu_1 - H\mathcal{W}_-N \left(\frac{\partial u_2}{\partial y} + \frac{\partial u_3}{\partial z} \right) = 0, \quad (2.48)$$

$$\nu \frac{\partial u_2}{\partial x} + \mathcal{W}_+ \left(\frac{\partial}{\partial y} \left(p - \mathcal{W}_+Nu_1 + \nu \left(\frac{\partial u_2}{\partial y} + \frac{\partial u_3}{\partial z} \right) \right) + Nu_2 \right) = 0, \quad (2.49)$$

$$\nu \frac{\partial u_3}{\partial x} + \mathcal{W}_+ \left(\frac{\partial}{\partial z} \left(p - \mathcal{W}_+Nu_1 + \nu \left(\frac{\partial u_2}{\partial y} + \frac{\partial u_3}{\partial z} \right) \right) + Nu_3 \right) = 0. \quad (2.50)$$

Construction of exact conditions on a spherical boundary has not, to our knowledge, been carried out. A closer study of the exact conditions in the planar case is quite suggestive of how these would look. Note, in particular, that (2.48) is related to the exact condition for the Laplace equation satisfied by p , namely $p_x + H^{-1}p = 0$. The other two conditions are related to the advection–diffusion equation for the vorticity. As the exact conditions on a sphere for the Poisson equation and the advection–diffusion equation are easily formulated, it is reasonable to believe that an exact condition for the Navier–Stokes equations can be similarly found and will involve the same nonlocal operators.

Exact boundary conditions for the compressible Navier–Stokes equations can be found using the same techniques as discussed by Halpern (1991) and Hagstrom and Lorenz (1994). In that case, the number of boundary conditions is different at inflow and outflow boundaries. In addition, nonlocal operators associated with the wave equation are involved.

3. Approximations and implementations

Having now completed an exhaustive study of exact boundary conditions for a wide class of problems of physical interest, we turn to the problem of efficient implementation of or approximation to the nonlocal operators appearing in our formulations. I will restrict attention to the scalar wave equation. As we have seen, exact conditions for most other important hyperbolic systems involve the same pseudodifferential operators, so the techniques we develop will be applicable in all these cases.

As mentioned earlier, it was generally believed that the direct implementation of the exact conditions is prohibitively expensive, a belief which discouraged their study. Considering flop counts, this belief is false. Hairer, Lubich and Schlichte (1985) present an algorithm for the fast solution of convolutional Volterra equations. Its application to the exact boundary conditions in integral form yields a method for which the computational effort is smaller than that required by the interior solver, except for unusually long times. However, this approach does require the storage of full time histories at the boundary, which is excessive for moderately long time simulations.

The primary alternative to direct implementation of the temporal integrals is the use of approximations to (or in the spherical case representations of) the kernels by sums of complex exponentials. For such kernels, convolution is equivalent to the solution of differential equations, so that the necessary work per time-step and storage is proportional to the number of exponentials used. In the next few sections I will develop the basic error estimates for such approximations and consider some examples. The same theory can be used to analyse the error associated with sponge layers, and I will do so for the so-called perfectly matched layer (PML), a reflectionless sponge layer recently introduced in computational electromagnetics.

3.1. Convolution with sums of complex exponentials

Consider the problem of computing

$$\mathcal{O}u \equiv \mathcal{H}^{-1} (E_l * (\mathcal{H}u)_l),$$

where now \mathcal{H} is any of the spatial harmonic transforms from the preceding sections, l is the harmonic index, $*$ is temporal convolution, and E_l takes the form

$$E_l(t) = \sum_{j=1}^{n_l} \alpha_{lj} e^{\beta_{lj}t}, \quad \text{Re } \beta_{lj} \leq 0. \quad (3.1)$$

Note that $\hat{E}_l(s)$ is a rational function of s of degree $(n_l - 1, n_l)$. There are two distinct and useful ways to represent \hat{E}_l . The first is as a sum of poles, which is directly derivable from (3.1):

$$\hat{E}_l(s) = \sum_{j=1}^{n_l} \frac{\alpha_{lj}}{s - \beta_{jl}}.$$

Then, for any function $w(t)$,

$$(E_l * w)(t) = \sum_{j=1}^{n_l} \phi_{lj}(t), \quad (3.2)$$

where the ϕ_{lj} satisfy the differential equations

$$\left(\frac{\partial}{\partial t} - \beta_{lj}\right)\phi_{lj} = \alpha_{lj}w, \quad \phi_{lj}(0) = 0.$$

The second representation is as a finite continued fraction,

$$\hat{E}_l(s) = \frac{\gamma_{l1}}{s + \delta_{l1} + \frac{\gamma_{l2}}{s + \delta_{l2} + \frac{\gamma_{l3}}{s + \dots}}}, \quad (3.3)$$

which is terminated by the condition

$$\gamma_{l, n_l+1} = 0.$$

Then, following Xu and Hagstrom (1999), Hagstrom and Hariharan (1998), we may evaluate $E_l * w$ in recursive form. In particular, set

$$\hat{E}_{lk}(s) = \frac{\gamma_{lk}}{s + \delta_{lk} + \frac{\gamma_{l, k+1}}{s + \delta_{l, k+1} + \frac{\gamma_{l, k+2}}{s + \delta_{l, k+1} + \dots}}} = \frac{\gamma_{lk}}{s + \delta_{lk} + \hat{E}_{l, k+1}},$$

where $\hat{E}_{l1} = \hat{E}_l$ and $\hat{E}_{l, n_l+1} = 0$. Set

$$w_k = \hat{E}_{lk} * w_{k-1}, \quad w_0 = w, \quad w_{n_l+1} = 0.$$

Then we have

$$\frac{\partial w_k}{\partial t} + \delta_{lk}w_k = \gamma_{lk}w_{k-1} - w_{k+1}, \quad k = 1, \dots, n_l. \quad (3.4)$$

Hence, for each representation, we must introduce n_l auxiliary functions for the l th harmonic for a total of

$$N_a = \sum_{l=0}^N n_l,$$

auxiliary functions where N is the number of harmonics used to represent the solution. The work per step and storage associated with the convolution is thus proportional (with a small constant) to N_a . Note that we must also apply the harmonic transform, \mathcal{H} , and its inverse at each step. In some instances this simply involves fast Fourier transforms, while in others we require spherical harmonic transforms using, for instance, the methods of Mohlenkamp (1997) and Driscoll, Healy and Rockmore (1997). In the former case the work is $O(N \ln N)$, but in the latter we have $O(N \ln^2 N)$.

In special cases, the harmonic transform phase of the application of the boundary condition can be avoided. This occurs when the constants α_{lj} , β_{lj} or γ_{lj} , δ_{lj} are eigenvalues of differential operators with eigenfunctions given by the l th harmonic. The most important example of this is the case of the exact boundary condition at a spherical boundary. Then (2.19) has the

form (3.3) with s replaced by Rs/c and

$$\begin{aligned}\gamma_1 &= \frac{l(l+1)}{2}, \\ \gamma_{lj} &= \frac{l(l+1) - (j-1)j}{4}, \quad j > 1, \\ \delta_{lj} &= j.\end{aligned}$$

Recalling that

$$\nabla_{\text{sphere}}^2 Y_l = -l(l+1)Y_l,$$

we see that for $k = 1, \dots, N$ (3.4) takes the form

$$\frac{1}{c} \frac{\partial w_k}{\partial t} + \frac{k}{R} w_k = -\frac{1}{4R^2} \left(\nabla_{\text{sphere}}^2 + k(k-1) \right) w_{k-1} - w_{k+1}, \quad (3.5)$$

with $w_0 = u/2$, $w_{N+1} = 0$. Then, if we assume

$$u = \sum_{l=1}^N u_l Y_l,$$

we have

$$w_1 = \frac{1}{R^2} \mathcal{H}^{-1} (S_l(ct/R) * (\mathcal{H}u)_l),$$

that is, w_1 is precisely the nonlocal part of (2.18). (Note: w_j as defined here differs from that in Hagstrom and Hariharan (1998) by a factor of $(-1)^j$.)

The recursive form above can also be modified for use in approximating the nonlocal terms in (2.22), as discussed by Hagstrom and Hariharan (1998), though the approximation is no longer exact. For different approaches to implementing (2.18), see Sofronov (1999) and Grote and Keller (1995, 1996). As these involve spherical harmonic transforms, I expect the formulation given here will be somewhat more efficient, and certainly much easier to implement. The derivation of the continued fraction form was inspired by the reformulation by Barry, Bielak and MacCamy (1988) of asymptotic boundary conditions based on progressive wave expansions first suggested by Bayliss and Turkel (1980). See Hagstrom and Hariharan (1996) for more details.

A different approach to applying approximate boundary conditions, based on localizable, homogeneous, rational approximations to the transformed representation of the exact boundary condition on a planar boundary (2.12), is developed in Higdon (1987, 1986). In particular, suppose that we approximate

$$\frac{|k|^2}{\tilde{s} + \sqrt{\tilde{s}^2 + |k|^2}} \approx \tilde{s}|k|^2 \sum_{j=1}^q \frac{\alpha_j}{\tilde{s}^2 + \beta_j^2 |k|^2}, \quad (3.6)$$

which is a general form for a homogeneous approximation that is localizable in time and space. Set

$$\lambda^2 = \tilde{s}^2 + |k|^2,$$

and note that, if u is a solution of the wave equation,

$$\lambda^2 \hat{u} = \frac{\partial^2 \hat{u}}{\partial x^2}.$$

Replacing $|k|^2$ by $\lambda^2 - \tilde{s}^2$ leads to a boundary condition of the form

$$\begin{aligned} Q(\tilde{s}, \lambda) \hat{u} &= 0, \\ Q(\tilde{s}, \lambda) &= (\tilde{s} + \lambda) \left(1 - \tilde{s}(\lambda - \tilde{s}) \sum_{j=1}^q \frac{\alpha_j}{(1 - \beta_j^2) \tilde{s}^2 + \beta_j^2 \lambda^2} \right). \end{aligned}$$

Multiplying through by the denominator and factoring the result we find that

$$\prod_{j=1}^{2q+1} (\eta_j \tilde{s} + \lambda) \hat{u} = 0,$$

which is equivalent to

$$\prod_{j=1}^{2q+1} \left(\frac{\eta_j}{c} \frac{\partial}{\partial t} + \frac{\partial}{\partial x} \right) u = 0. \quad (3.7)$$

Stably implementing boundary conditions in this form is a reasonably simple matter. However, it may not be feasible to choose q very large (as is my intent) due to the growth of the difference stencil into the interior domain, so that I generally use auxiliary functions as in (3.2) or (3.4). Starting from (3.7), the parameters η_j , which typically correspond to cosines of incidence angles of perfect absorption, may be adjusted directly. This formulation has been applied in a number of more complex settings by Higdon (1991, 1992, 1994).

3.2. Stability and consistency

Error estimates are derived, as always, by establishing the stability and consistency of the approximate boundary conditions. Let us begin with the simplest case of a planar boundary and an approximate boundary condition defined by

$$\frac{|k|^2}{\tilde{s} + \sqrt{\tilde{s}^2 + |k|^2}} \approx |k| \hat{R}(\tilde{s}, k).$$

Assume further, for simplicity, that Υ is the half-space $x < 0$. Then the Fourier–Laplace transform of the exact solution, u , and the error, e , take

the form

$$\hat{u} = Ae^{-\sqrt{\tilde{s}^2 + |k|^2}x}, \quad \hat{e} = Ee^{\sqrt{\tilde{s}^2 + |k|^2}x},$$

with the amplitudes related by

$$E = \frac{\tilde{s} + |k|\hat{R} - \sqrt{\tilde{s}^2 + |k|^2}}{\tilde{s} + |k|\hat{R} + \sqrt{\tilde{s}^2 + |k|^2}}A \equiv \epsilon(\tilde{s}, |k|)A. \quad (3.8)$$

(Generally, for more realistic choices of Υ , e must satisfy homogeneous boundary conditions on Σ , and so has a more complicated form. However, similar error estimates can be derived.) By Parseval's relation we find, on bounded subsets $\Upsilon' \subset \Upsilon$:

$$\|e\|_{L_2(0,T;L_2(\Upsilon'))} \leq C(\Upsilon') \left(\int e^{2\eta(k)T} \sup_{\text{Re } s = \eta(k)} |\epsilon|^2 \|\bar{u}(0, k, \cdot)\|_{L_2(0,T)}^2 dk \right)^{1/2}.$$

To bound $|\epsilon|$, we must derive an upper bound on its numerator (consistency), and a lower bound on its denominator (stability). It is interesting to note that if we replace the approximate boundary condition by the exact boundary condition, the denominator has zeroes at $\tilde{s} = \pm i|k|$. Of course the numerator is identically zero in this case, so the error is indeed zero. However, we expect that accurate approximate conditions will have small denominators near these points. A simple sufficient condition for stability is

$$\text{Re } \hat{R} > 0, \quad \text{Re } s \geq 0. \quad (3.9)$$

This can be relaxed somewhat, as will be seen in one of the examples.

Ideally, we would take $\eta = 0$ so that our estimates are uniform in time. However, stable, homogeneous spatially localizable conditions generally have poles on the imaginary s axis. (See Trefethen and Halpern (1986, 1988).) At such points $|\epsilon| \geq 1$, so that no useful estimate holds. Therefore, for spatially local conditions we generally must settle for finite time estimates.

In numerical calculations we can only treat functions with wave numbers in some bounded set, $|k| \leq M$. Our error analysis simplifies somewhat if we restrict our attention to this set. The accuracy of any method is then characterized by

$$\delta(T, M; \hat{R}) = \sup_{|k| \leq M} \inf_{\eta \geq 0} \sup_{\text{Re } s = \eta} e^{\eta T} |\epsilon|. \quad (3.10)$$

Alternatively, we can seek estimates involving derivative norms of the solution, leading to error estimates in terms of

$$\sup_{|k| \leq M} \inf_{\eta \geq 0} \sup_{\text{Re } s = \eta} e^{\eta T} (1 + |k|^2)^{-\mu/2} |\epsilon|.$$

In this exposition I will follow the former, simpler approach. For examples of the latter see Hagstrom (1995, 1996) and Xu and Hagstrom (1999).

The analysis outlined above is easily extended to our other special boundaries. For example, suppose Υ is the sphere of radius R and the approximate boundary condition is defined by

$$\hat{S}_l(R\tilde{s}) \approx \hat{V}_l(\tilde{s}, R).$$

Then

$$\hat{e}_l = \epsilon_l(\tilde{s}, R) \hat{u}_l(\tilde{s}, R) \sqrt{\frac{R}{\rho} \frac{I_{l+1/2}(\rho\tilde{s})}{I_{l+1/2}(R\tilde{s})}},$$

where $I_{l+1/2}$ is the modified Bessel function of the first kind (Abramowitz and Stegun 1972, Ch. 9), and ϵ_l is given by

$$\frac{\hat{V}_l - \hat{S}_l}{R^2 \frac{\partial}{\partial \rho} \left(\sqrt{\frac{R}{\rho}} \frac{I_{l+1/2}(\rho\tilde{s})}{I_{l+1/2}(R\tilde{s})} \right) \Big|_{\rho=R + \tilde{s}R^2 + R + \hat{V}_l}}. \quad (3.11)$$

The accuracy of the method may then be characterized by the obvious analogue of (3.10).

In the following sections I will estimate δ for various approximations.

3.3. Padé approximants and generalizations

For planar boundaries the function $\hat{R}(\tilde{s}, |k|)$ approximates the function

$$\hat{K}(z) = (z + \sqrt{z^2 + 1})^{-1}$$

with $z = \tilde{s}/|k|$. Let $\hat{R}_p(z)$ be some approximation to \hat{K} . Noting that

$$\hat{K} = \frac{1}{2z + \hat{K}},$$

it is reasonable to set

$$\hat{R}_{p+1} = \frac{1}{2z + \hat{R}_p}. \quad (3.12)$$

Approximations based on (3.12) are extensively analysed in Xu and Hagstrom (1999). It is clear that they are in continued fraction form, and hence implementable via the recursion (3.4). Precisely,

$$\gamma_1 = \frac{|k|^2}{2}, \quad \gamma_j = \frac{|k|^2}{4}, \quad k = j, \dots, n_l,$$

$$\delta_j = 0, \quad j = 1, \dots, n_l - 1, \quad \delta_{n_l} = |k| \hat{R}_0.$$

Note that

$$\hat{R}_{p+1} - \hat{K} = \frac{\hat{K} - \hat{R}_p}{(2z + \hat{K})(2z + \hat{R}_p)}.$$

Therefore, if we assume that \hat{R}_p is at least bounded as $z \rightarrow \infty$, we gain two orders in the large z approximation at each step. That is,

$$|\hat{R}_{p+1} - \hat{K}| = O(z^{-2})|\hat{R}_p - \hat{K}|.$$

Consider the initialization

$$\hat{R}_0 = a \geq 0.$$

Then an easy induction argument shows that $\text{Re } \hat{R}_p > 0$ when $\text{Re } z > 0$ and that all poles are in the closed left half-plane. For $a > 0$, we can further conclude that the poles and zeroes of the real part lie in the open left half-plane. The choice $a = 0$, however, leads to the Padé approximants introduced by Engquist and Majda (1977) and Lindman (1975). These are spatially localizable, with poles on the imaginary z axis between $\pm i$.

Xu and Hagstrom (1999) show that \hat{R}_p is given by the following explicit formula:

$$\hat{R}_p = \frac{b^{2n+1} - (-1)^n b + a(b^{2n} + (-1)^n b^2)}{b^{2n+2} + (-1)^n + a(b^{2n+1} - (-1)^n b)}, \quad b = \frac{\tilde{s} + \sqrt{\tilde{s}^2 + |k|^2}}{|k|},$$

which leads to the remarkably simple formula for ϵ :

$$\epsilon(\tilde{s}, |k|) = (-1)^{n+1} \frac{1 - ab}{b^{2n+1}(b + a)}. \tag{3.13}$$

From this we derive the following theorem.

Theorem 1 Let $a \geq 0$ and $\eta, M > 0$ be given. Then,

$$\sup_{\text{Re } s = \eta, |k| \leq M} |\epsilon| \leq (1 + a) \left(1 + 2 \frac{\eta^2}{c^2 M^2} \right)^{-(n+1/2)}.$$

The proof of this theorem follows immediately from the inequality

$$\inf_{\text{Re } z = \eta} |b| \geq \sqrt{1 + 2\eta^2}.$$

From the estimate it might be concluded that the Padé approximants, $a = 0$, are optimal in this class. However, we have proceeded crudely. The minimum of $|b|$ leading to the inequality above occurs at $\text{Im } z = 0$ where we can force $\epsilon = 0$ by a proper choice of a . A more detailed analysis is given in Xu and Hagstrom (1999).

Imposing a tolerance τ and a computation time T we require

$$\delta(T, M) < \tau,$$

which implies

$$n + \frac{1}{2} > \frac{\ln \frac{1+a}{\tau} + \eta T}{\ln \left(1 + 2 \frac{\eta^2}{c^2 M^2} \right)}.$$

Optimizing this over η yields (for cMT on the order of $\ln 1/\tau$) the following result.

Theorem 2 For any $0 \leq a \leq 1$ there exists a constant, C , such that for any tolerance $0 < \tau < 1$, wave number bound M , and time $T > 0$, the approximation \hat{R}_p with

$$p > C \left(\ln \frac{1}{\tau} + cMT \right),$$

satisfies $\delta(T, M; \hat{R}_p) < \tau$.

We see that the number of terms required is weakly dependent on the tolerance, but strongly dependent on the time and the tangential wave numbers.

A completely different convergence analysis for the Padé approximants was given in Hagstrom (1995), with the same conclusions. Many other space-time localizable conditions are proposed in Trefethen and Halpern (1988), whose accuracy has not, to my knowledge, been estimated.

3.4. Truncations of (2.19) and asymptotic boundary conditions

A second approach to the construction of local approximate boundary conditions has been through the use of the progressive wave expansion, given in the cylindrical case by

$$u \sim \sum_{j=0}^{\infty} r^{-j-\frac{1}{2}} f_j(ct - r, \theta), \quad (3.14)$$

and in the spherical by

$$u \sim \sum_{j=0}^{\infty} r^{-j-1} f_j(ct - r, \theta, \phi), \quad (3.15)$$

where for notational convenience we now use r instead of ρ to denote the spherical radius. (For a mathematical discussion of expansions of this type see Ludwig (1960).)

These are used by Bayliss and Turkel (1980) to construct a hierarchy of boundary conditions satisfied by truncations of the expansion. This is easily accomplished using normal derivatives:

$$B_p(B_{p-1}(\cdots(B_1 u))) = 0,$$

$$B_p = \left(\frac{1}{c} \frac{\partial}{\partial t} + \frac{\partial}{\partial r} + \frac{2(p-1) + \alpha}{R} \right),$$

where $\alpha = 1/2$ for (3.14) and $\alpha = 1$ for (3.15). However, the product form limits the order, p , which can be practically used. An alternative proposed by Hagstrom and Hariharan (1998) is to use the continued fraction form

(2.19) or its cylindrical analogue, which has the form (3.3) with s replaced by Rs/c and

$$\begin{aligned}\gamma_{l1} &= \frac{l^2 - 1/4}{2}, \\ \gamma_{lj} &= \frac{l^2 - (j - 1/2)^2}{4}, \quad j > 1, \\ \delta_{lj} &= j.\end{aligned}$$

Here, l is the dual Fourier variable to θ .

Truncating the expansions after $p - 1$ terms, that is, setting $w_p = 0$, leads to an approximate boundary condition whose accuracy may be assessed, in the spherical case, via (3.11). We have not carried through this analysis in full detail, as in the preceding section. However, we can make some conclusions.

Assume $l \gg p$. We then rely on the uniform large index asymptotic expansions for Bessel functions developed by Olver (1954). In particular, we find, to leading order, that away from the transition zones $R\tilde{s} \approx \pm il$

$$\frac{\tilde{s}k'_l(R\tilde{s})}{k_l(R\tilde{s})} \sim -\sqrt{\tilde{s}^2 + \frac{l^2}{R^2}},$$

which obviously corresponds to the planar case. By direct computation we see that the approximate boundary condition poorly approximates the exact condition when

$$\frac{l}{R} \gg |\tilde{s}|. \quad (3.16)$$

For $|\tilde{s}| \gg l/R$, on the other hand, the approximation is good. Here, instead of increasing the order of the boundary condition, we can expand the domain, moving the boundary to γR . Evaluating the error on the original domain only, we see that our expression for ϵ picks up an extra factor of

$$\frac{K_{l+1/2}(\gamma R\tilde{s})}{K_{l+1/2}(R\tilde{s})} \cdot \frac{I_{l+1/2}(R\tilde{s})}{I_{l+1/2}(\gamma R\tilde{s})}.$$

Assuming (3.16), this factor is approximately γ^{-2l} . Therefore, we may hope that the error is small if γ^{-2p} is small, which requires

$$\gamma > \left(\frac{1}{\tau}\right)^{\frac{1}{2p}}.$$

Clearly, this argument is far from a proof. In particular we have completely ignored the transition regions. Their analysis might introduce some time dependence in the estimates, as in the similar case of the Padé approximants. We find that, with these favourable assumptions, some improve-

ments can be made by combining domain extension with increases in p . It is therefore of some interest to carry through the convergence analysis.

3.5. Uniform rational approximants

The analysis above points to a defect of the continued fraction approximations, namely, poor approximation properties for tangential wave numbers which are large in comparison to s . This suggests that substantial improvements can be made by uniformly approximating the transforms of the exact boundary kernels along lines $\text{Re } s = \eta \geq 0$.

This program is carried out in Alpert *et al.* (1999b). It consists of two parts: proofs using multipole theory that good approximations exist, followed by the numerical construction of the poles and coefficients via non-linear least squares. The fundamental approximation theorems used, which follow from the methods of Anderson (1992) and are proven in Alpert *et al.* (1999b), can be summarized in the following form.

Theorem 3 Suppose D_i , $i = 1, \dots, p$ are disks in the complex plane of radius r_i and centre c_i . Suppose the complex numbers z_j , $j = 1, \dots, n$, and curve, C , lie within the union of the disks and that the function $f(z)$ is defined by

$$f(z) = \sum_{j=1}^n \frac{q_j}{z - z_j} + \int_C \frac{q(\zeta)}{z - \zeta} d\zeta.$$

Then there exists a rational function $g_m(z)$ with mp poles, all lying on the boundaries of the D_i , such that for any z satisfying $\text{Re}(z - c_i) \geq ar_i > r_i$, $i = 1, \dots, p$,

$$|f(z) - g_m(z)| \leq \frac{2(a^2 + 1)}{(a^m - 1)(a - 1)^2} |F(z)|,$$

where

$$F(z) = \sum_{j=1}^n \frac{|q_j|}{z - z_j} + \int_C \frac{|q(\zeta)|}{z - \zeta} d\zeta.$$

The proof follows from the direct construction of g_m . One simply places poles symmetrically around the boundary of the disks with coefficients chosen to match the large z expansion of each disk's contribution to f .

The application of Theorem 3 to the approximation of $\hat{S}_l(z)$ is quite direct. As \hat{S}_l is a rational function, it can be written as a sum of poles. These poles are zeroes of $K_{l+1/2}(z)$, and uniform large l expansions of their locations are given in Olver (1954). In particular, they lie near a curve in the left half z -plane connecting the points $z = \pm il$, with the poles nearest the imaginary axis separated from it by an $O(l^{1/3})$ distance. We cover these poles by $O(\ln l)$ disks such that all points in the closed right half z -plane satisfy the

Table 1. Number of poles, p , required to approximate \hat{S}_l , $l \leq M$, with $\delta(T, M) < \tau$

τ	$M = 128$	$M = 256$	$M = 512$	$M = 1024$
10^{-6}	12	14	15	16
10^{-8}	16	17	19	21
10^{-15}	26	29	33	36

inequality $\operatorname{Re}(z - c_i) \geq 2r_i$. Using $m \cdot O(\ln l)$ we thus achieve an error that scales like 2^{-m} . Taking into account the behaviour of the denominator of (3.11) near $z = \pm il$, we deduce that, for some l -independent constant C ,

$$|\epsilon_l| \leq Cl^{1/3}2^{-m}.$$

Hence we have the following theorem.

Theorem 4 There exists a constant C such that, for any tolerance $0 < \tau < 1$, wave number bound $M > 1$, radius $R > 0$, and time $T > 0$, there exists a p -pole rational approximation $\hat{P}_l(z)$ with

$$p < C \cdot \ln M \cdot \left(\ln \frac{1}{\tau} + \ln M \right),$$

such that $\delta(T, M; \hat{P}_l) < \tau$.

Note that the number of poles required is bounded independent of T . We have numerically constructed approximations satisfying Theorem 4. The number of poles required as M and τ are varied are listed in Table 1. One cannot but be impressed by the efficiency of these approximations, which allow the evaluation of the exact condition for harmonics of index up to 1024 to double precision accuracy with no more than 36 poles per harmonic.

It is also possible to apply Theorem 3 to the approximation of the transform of the cylindrical kernel, \hat{C}_l , and the planar kernel, \hat{K} . In each case we use integral representations of the form given in the theorem. Details in the cylindrical case for $k_z = 0$ are given in Alpert *et al.* (1999b), while the planar case will be discussed elsewhere. Both \hat{C}_0 and \hat{K} have branch points on the imaginary axis. This forces us to settle for approximations with $\operatorname{Re} s \geq \eta > 0$. The number of poles required will thus depend on the time, T , as well as on M and τ . For the planar case we have the following theorem.

Theorem 5 There exists a constant C such that, for any tolerance $0 < \tau < 1$, wave number bound M , and time T such that $cMT > 2$, there exists

a p -pole rational approximation $\hat{R}(s, k)$ with

$$p < C \cdot \ln cMT \cdot \left(\ln \frac{1}{\tau} + \ln cMT \right),$$

such that $\delta(T, M; \hat{R}) < \tau$.

The planar approximations are computed by specifying τ and $\eta = (MT)^{-1}$. Choosing $\tau = 10^{-3}$ and $\eta = 10^{-4}$ leads to a 21-pole approximation which is used in the numerical experiments below.

3.6. Reflectionless sponge layers

An alternative to the imposition of radiation boundary conditions at the artificial boundary is to surround the computational domain Υ with a sponge layer or absorbing region, within which propagating waves are damped. Though the construction of layers that absorb wave energy is reasonably simple, additional errors are typically introduced by the interaction of waves with the interface between the computational domain and the layer. Recently this approach was revitalized by the construction in Berenger (1994) of a sponge layer for Maxwell's equations with a reflectionless interface: the so-called *perfectly matched layer*, or PML. As shown in Abarbanel and Gottlieb (1997), the original formulation is only weakly well-posed. Petropoulos (1999) gives a clear mathematical derivation of reflectionless sponge layers in Cartesian, cylindrical and spherical coordinates, and derives strongly well-posed formulations.

Surprisingly, much less has been written about reflectionless sponge layers for the wave equation. Here I adapt the construction of Chew and Weedon (1994) and Petropoulos (1999) to the wave equation and analyse the error, restricting myself to the planar case. The error estimates thus derived coincide with those derived for Maxwell's equations by the same techniques.

Take x to be the coordinate normal to the layer interface and suppose that Υ corresponds to $x < 0$. The simplest starting point for the analysis is at the level of the solutions in Υ , described after our usual Fourier–Laplace transformation by

$$\hat{u} = e^{\pm \sqrt{\tilde{s}^2 + |k|^2} x}.$$

Clearly, these solutions are not damped with increasing or decreasing x for imaginary \tilde{s} satisfying $|\tilde{s}| \geq |k|$, that is, for propagating modes. Damping may be achieved by modifying the exponent so that it has a real part that decreases with increasing x for the right-propagating (–) mode, and increases with increasing x for the left-propagating mode. As the sign of the imaginary part of $\sqrt{\tilde{s}^2 + |k|^2}$ coincides with that of \tilde{s} in the propagating mode regime, this is accomplished by adding to x an increasing in x imaginary function whose imaginary part has the opposite sign from that of \tilde{s} . A

simple function with this property is

$$\frac{\int_0^x \tilde{\sigma}(w) dw}{\tilde{s}}, \quad \tilde{\sigma} \geq 0.$$

Thus we seek solutions in the sponge layer in the form

$$\hat{u} = e^{\pm \sqrt{\tilde{s}^2 + |k|^2}(x + \tilde{s}^{-1} \int_0^x \tilde{\sigma}(w) dw)}.$$

The interface $x = 0$ will be reflectionless if the solutions and their x -derivatives coincide there. This imposes the additional constraint

$$\tilde{\sigma}(0) = 0.$$

This constraint is not present in applications to hyperbolic systems, but is almost always imposed in computations. No other conditions on $\tilde{\sigma}$ are needed to make the interface reflectionless.

From the layer solutions it is straightforward to derive a pseudodifferential equation. For \hat{u} we have

$$\tilde{s}^2 \hat{u} = \frac{\tilde{s}}{\tilde{s} + \tilde{\sigma}} \frac{\partial}{\partial x} \left(\frac{\tilde{s}}{\tilde{s} + \tilde{\sigma}} \frac{\partial \hat{u}}{\partial x} \right) - |k|^2 \hat{u}.$$

Inverting the transforms, introducing $\sigma = c\tilde{\sigma}$, and assuming zero initial data in the layer, we finally obtain

$$\frac{1}{c^2} \frac{\partial^2 u}{\partial t^2} = (1 - \sigma(x)\mathcal{I}*) \frac{\partial}{\partial x} \left((1 - \sigma(x)\mathcal{I}*) \frac{\partial u}{\partial x} \right) + \nabla_y^2 u, \quad (3.17)$$

where

$$\mathcal{I} * w = \int_0^t e^{-\sigma(x)(t-\tau)} w(\tau) d\tau.$$

Local implementations involve the introduction of auxiliary variables to eliminate the convolutions. It is here that strong well-posedness can be lost. In our numerical experiments we replace (3.17) by

$$\frac{1}{c^2} \frac{\partial^2 u}{\partial t^2} = \nabla^2 u - \frac{\partial v}{\partial x} - w, \quad (3.18)$$

$$\frac{\partial v}{\partial t} + \sigma v = \sigma \frac{\partial u}{\partial x}, \quad (3.19)$$

$$\frac{\partial w}{\partial t} + \sigma w = \sigma \frac{\partial^2 u}{\partial x^2} - \sigma \frac{\partial v}{\partial x}. \quad (3.20)$$

These are strongly well-posed, but possibly not asymptotically stable, so that other reformulations may be better.

To complete the layer description we must specify its length, d , and impose a boundary condition at its edge. Here I make the simplest choice,

$u = 0$, though of course one could lower the error with more sophisticated conditions. The general solution within the layer is then given by

$$\hat{u} = A_l \left(e^{-\sqrt{\tilde{s}^2 + |k|^2}((x-d) + \tilde{s}^{-1} \int_d^x \bar{\sigma}(w) dw)} - e^{\sqrt{\tilde{s}^2 + |k|^2}((x-d) + \tilde{s}^{-1} \int_d^x \bar{\sigma}(w) dw)} \right).$$

Matching this to a solution in Υ of the form

$$Ae^{-\sqrt{\tilde{s}^2 + |k|^2}x} - Ee^{\sqrt{\tilde{s}^2 + |k|^2}x},$$

we find that E is related to A as in (3.8) with

$$\epsilon(\tilde{s}, |k|) = e^{-2\sqrt{\tilde{s}^2 + |k|^2}(d + \tilde{s}^{-1} \int_0^d \bar{\sigma}(w) dw)}.$$

We see that, as in the case of rational approximants to \hat{K} , good error estimates do not hold along the imaginary \tilde{s} axis, particularly near $\tilde{s} = \pm i|k|$. Taking $\text{Re } s = \eta > 0$ and introducing $\bar{\sigma} = d^{-1} \int_0^d \bar{\sigma}(w) dw$, we must estimate

$$\min_{\text{Re } z = \frac{\eta}{c|k|}} \text{Re} \left(2d\sqrt{z^2 + 1}(|k| + z^{-1}\bar{\sigma}) \right). \quad (3.21)$$

Consider the case of $\tilde{\eta} \equiv \frac{\eta}{c|k|} \ll 1$. Writing $z = \tilde{\eta} + i\zeta$, we find the quantity to be minimized in (3.21) to be approximated by

$$2d\sqrt{1 - \zeta^2}(|k| + \tilde{\eta}\bar{\sigma}/(\tilde{\eta}^2 + \zeta^2)), \quad |\zeta| < 1,$$

$$2d\sqrt{\zeta^2 - 1} \bar{\sigma} |\zeta|^{-1}, \quad |\zeta| > 1,$$

$$2d \text{Re} \left(\sqrt{2(1 - |\zeta| \pm i\tilde{\eta})}(|k| \mp i\bar{\sigma}) \right), \quad \zeta \approx \pm 1.$$

Hence, for $\tilde{\eta}$ sufficiently small, the minimum is achieved near $|\zeta| = 1$. Restricting $\tilde{\eta}$ to be no greater than one, we have, for some constant C ,

$$\delta \leq e^{\tilde{\eta}c|k|T - Cd\sqrt{\tilde{\eta}}(|k| + \bar{\sigma})}.$$

Minimizing over $\tilde{\eta}$ and maximizing over $|k|$ we prove the following.

Theorem 6 There exists a constant C such that, for any tolerance $0 < \tau < 1$, wave number bound, M , and time, T , the ideal reflectionless sponge layer (3.17) with average absorption $\bar{\sigma} > 0$ and width, d , satisfying

$$d\bar{\sigma} \geq C \left(\sqrt{c\bar{\sigma}T} + \sqrt{\ln \frac{1}{\tau}} \right) \cdot \sqrt{\ln \frac{1}{\tau}},$$

will have $\delta(T, M) < \tau$.

A remarkable feature of this bound is its independence of the maximum wave number, M .

3.7. Complexity

Armed with these error estimates, we are in a position to assess the relative efficiency of the various accurate approaches. We consider two distinct idealized problems governed by the wave equation, with units chosen so that $c = 1$. The first problem assumes a three-dimensional computational domain Υ that is 1-periodic in two coordinate directions, has length 1 in the third direction, and is truncated by an artificial boundary at each end. The second problem assumes that Υ is contained within a sphere of radius 1, which serves as the artificial boundary. The first problem is used to test conditions for periodic or waveguide problems and the second to test conditions for exterior problems. In practice, planar boundaries are used to solve exterior problems, enclosing the computational domain in a box. Unfortunately, we do not as yet have any hard error estimates for either the Padé approximants or reflectionless sponge layers used in this way, and so can only make conjectures concerning their efficiency.

In each case we assume that wave numbers up to M must be resolved on the boundary and that we are interested in the solution up to time T . We also suppose that the error tolerance is τ . For purposes of comparison it is useful to note the work, W_I , and storage, S_I , required by the interior solver. Assuming an explicit method with reasonable stability constraint, these are

$$W_I \propto \alpha^4 M^4 T, \quad S_I \propto \alpha^3 M^3,$$

where α is the number of points per wavelength. Appropriate values for α are strongly dependent on the order of the method and may also depend on T . It will also be proportional to $\tau^{-1/p}$ for a p th order method. In what follows I will suppress the α dependence, but it should then be kept in mind that in some instances α can be fairly large, and some methods will allow coarser representations when evaluating the boundary conditions. Similarly, we will treat logarithmic dependences on the tolerance as $O(1)$ constants.

I have tried to keep the analysis as simple as possible, ignoring possible improvements in the complexity estimates that might be achievable by better implementations. Of course I hope that in the future this analysis will be supplemented by serious computational experimentation.

Domain extension

By far the simplest way to achieve an accurate solution is to exploit the finite signal speed and extend the domain so that the boundary cannot influence the solution in Υ for times less than T . Clearly this requires an extension of width $O(T)$. For the first problem the volume of the extended region is proportional to T so that the extra work and storage, which we shall always denote by W_B and S_B , is given by

$$W_B \propto M^4 T^2, \quad S_B \propto M^3 T.$$

We see that the work and storage exceeds that required by the interior scheme by a factor of T , which is clearly unacceptable for moderate to large times.

The results for the second problem are even worse, as the volume of the extension is proportional to T^3 , that is,

$$W_B \propto M^4 T^4, \quad S_B \propto M^3 T^3,$$

a factor of T^3 above the interior scheme.

Kirchoff's formula

Here we assume two spherical boundaries separated by a small distance. To compute the solution at each point on the outer boundary requires the computation of an integral over a sphere. This involves $O(M^4)$ work per time-step. Although it is reasonable to assume that the integration can be carried out on a coarser grid than required by the solution of the wave equation, so that the constant of proportionality may be small, the order estimates are

$$W_B \propto M^5 T, \quad S_B \propto M^3.$$

We see that the storage required is comparable to (probably less than) S_I but that the work is greater by a factor of M .

Direct implementation of the planar exact condition

Here we require direct and inverse Fourier transforms at each time step as well as the solution of the convolutional Volterra equation for each mode. Making use of the FFT, the work associated with the transformations is seen to be $O(M^2 \ln M)$ per time-step. For the convolution we may use the algorithm presented in Hairer *et al.* (1985), which requires $O(MT \ln^2 MT)$ operations per mode. As for storage, the direct implementation requires full storage of the time histories of the Fourier coefficients. This could probably be reduced somewhat using the $t^{-3/2}$ decay of the convolution kernel, $K(t)$, but I have not quantified the effect. Therefore we have

$$W_B \propto M^3 T \ln^2 MT, \quad S_B \propto M^3 T.$$

Except for extraordinarily long times, W_B compares favourably with W_I . However, we generally have $S_B > S_I$, possibly much greater for large T .

Direct implementation of the spherical exact condition

Here I will consider the completely local version (3.5). The implementations of Grote and Keller (1995, 1996) and Sofronov (1999) require an additional direct and inverse spherical harmonic transform per time-step. Using the fast algorithms of Driscoll *et al.* (1997) and Mohlenkamp (1997), this requires

$O(M^2 \ln^2 M)$ work per step and does not increase the order of the complexity estimate.

We require, then, the solution of M additional equations on the boundary, associated with M auxiliary variables. This costs

$$W_B \propto M^4 T, \quad S_B \propto M^3.$$

Here we have, taking account of the probable smaller proportionality constants due to the effect of α , $W_B \leq W_I$, $S_B \leq S_I$: the first method we have seen that meets our goals of arbitrary accuracy without increase in cost!

Padé approximants

Suppressing the weak dependence on the error tolerance, we require $O(MT)$ auxiliary functions and equations on the boundary. The cost then is

$$W_B \propto M^4 T^2, \quad S_B \propto M^3 T.$$

This is more by a factor of T than what is required by the interior solver, and so is unacceptable for long time computations. We note that in our numerical experiments the growth in the number of terms required as T increases was fairly mild, so that we expect the proportionality constants to be small.

High-order conditions based on the Padé approximants have been implemented on rectangular domains. This depends on remarkable constructions of corner compatibility conditions given by Collino (1993) and Vacus (1996). It would be of interest to extend the error estimates to this case. It is conceivable that they will be somewhat better, as glancing modes which reflect off one boundary may be effectively absorbed at near normal incidence by another.

Asymptotic boundary conditions

In this case we have no proven error estimates. Accepting the optimistic assumption that we must expand the domain by a factor of $\tau^{-1/(2p)}$, we find

$$W_B \propto (\tau^{-\frac{3}{2p}} - 1)M^4 T + pM^3 T, \quad S_B \propto (\tau^{-\frac{3}{2p}} - 1)M^3 + pM^2.$$

These estimates are optimized by

$$p \propto \sqrt{\ln \frac{1}{\tau}} \cdot M^{1/2},$$

which leads to work and storage estimates that are better than those obtained for the exact condition, $p = M$, in some cases. Clearly it would be of interest to make the error estimates precise.

Uniform rational approximants

These have been constructed for both planar and spherical boundaries, and hence are directly applicable to both problems. In the first case we require $O(\ln^2 MT)$ auxiliary functions per mode on the boundary, and direct and inverse Fourier transforms each time-step. Therefore the work and storage required are

$$W_B \propto M^3 T \ln^2 MT, \quad S_B \propto M^2 \ln^2 MT.$$

Except for extraordinarily long times, we have $W_B \ll W_I$ and $S_B \ll S_I$, so that the method fully satisfies our goals.

The situation in the spherical case is even better, at least so far as the time dependence of the estimates is concerned. We require $O(\ln^2 M)$ auxiliary functions per mode on the boundary and direct and inverse spherical harmonic transforms. Assuming we use the fast transforms alluded to above, the work and storage are

$$W_B \propto M^3 T \ln^2 M, \quad S_B \propto M^2 \ln^2 M.$$

Theoretically, then, the uniform approximants represent a completely acceptable solution to the boundary condition problem in the constant coefficient case for exterior problems, as they provide essentially arbitrary accuracy for arbitrary times with $W_B \ll W_I$ and $S_B \ll S_I$. There are some practical issues concerning the efficiency of the fast spherical harmonic transforms and the necessity of using an aspect ratio one computational domain.

Reflectionless sponge layers

Here there are two parameters, the layer width d and the average absorption, $\bar{\sigma}$. Clearly, the number of mesh points in the layer will scale like dM^3 with d in the planar case. Also, following the analysis in Collino and Monk (1998), the mesh spacing must scale inversely with $\bar{\sigma}$. Hence we will take $\bar{\sigma}$ fixed and reduce the error by increasing d . As $d \propto \sqrt{T}$ this implies

$$W_B \propto M^4 T^{3/2}, \quad S_B \propto M^3 T^{1/2},$$

which is unacceptable for large T .

Most practical applications of this technique involve exterior problems with a computational domain which is a box. Therefore, I believe it would be of great interest to extend the error estimates to this case. If the time dependence of the errors were as bad as in the planar case, then the long time behaviour would be even worse, as the volume of the layer would grow like $d^3 \propto T^{3/2}$. However, there is some reason to believe that far better estimates hold. This is due to the fact that glancing waves at one boundary are nearly normally incident to another, and hence should be effectively absorbed.

An alternative for exterior problems is the spherical layer developed in Petropoulos (1999). I believe that this layer could be directly analysed as a straightforward extension of the analysis given here. However, for problems of near unit aspect ratio, it is doubtful that a layer technique could be more efficient than the uniform rational approximants.

3.8. A numerical example

We now consider a simply described yet, as we shall see, difficult-to-solve concrete problem to illustrate some of our results. In particular, we solve the initial value problem for the wave equation in the planar region $(x, y) \in (-1, 1) \times (0, 1)$, assuming periodicity in y . An exact solution, $u(x, y, t)$, is constructed by setting off periodic arrays of pulses at various negative times. This leads to

$$u(x, y, t) = \sum_{i=1}^{n_{\text{pulse}}} u_i(x, y, t),$$

where

$$u_i(x, y, t) = \sum_{k=-\infty}^{\infty} \int_{-\infty}^{t-r_{ik}} \frac{\sigma_i(s)}{\sqrt{(t-s)^2 - r_{ik}^2}} ds$$

and

$$r_{ik}^2 = (x - x_i)^2 + (y - y_i - k)^2, \quad \sigma_i(s) = A_i e^{-\mu_i(s-\tau_i)^2}.$$

Here, $\tau_i < 0$ is chosen so that $A_i e^{-\mu_i \tau_i^2}$ is negligibly small. At $t = 0$ the solution is made negligibly small (to more than 11 digits) outside Υ . A program that accurately evaluates u using high-order Gaussian quadrature and high-order end-point corrected trapezoidal formulas for singular integrals was generously provided by Leslie Greengard, and is used to produce the error tables listed below. I am confident that the accuracy of the evaluation is on the order of ten decimal digits and, hence, far exceeds that of the numerical solutions.

These solutions were used to test Padé approximants of \hat{K} in numerical solutions of the linearized Euler equations (Hagstrom and Goodrich 1998) and will be used in the extensive numerical experiments to be presented in Alpert *et al.* (1999a). Here we consider a single pulse with parameters:

$$\mu_1 = 150, \quad \tau_1 = -\frac{1}{2}, \quad x_1 = 0, \quad y_1 = \frac{1}{2}, \quad A_1 = 1.$$

Three types of approximate boundary conditions were considered: the Padé sequence, using (3.12) with $\hat{R}_0 = 0$, and its generalization, (3.12) with $\hat{R}_0 = 1$; a strongly well-posed local implementation of the PML; and the planar uniform approximant computed with $\epsilon = 10^{-3}$ and $\eta = 10^{-4}$. The latter employs 21 poles. The approximate conditions are imposed at $x = \pm 1$. We

Table 2. *Errors using (3.12)*

\hat{R}_0	p	Max. err. $t \leq 5$	Max. err. $t \leq 25$	Max. err. $t \leq 50$
	0	1.2×10^{-1}	2.1×10^{-1}	2.1×10^{-1}
0	5	9.9×10^{-3}	7.0×10^{-2}	7.6×10^{-2}
0	10	1.2×10^{-3}	3.3×10^{-2}	5.5×10^{-2}
0	15	2.6×10^{-4}	1.9×10^{-2}	3.7×10^{-2}
0	20	1.5×10^{-4}	1.0×10^{-2}	2.9×10^{-2}
0	25	1.5×10^{-4}	6.4×10^{-3}	1.9×10^{-2}
0	30	1.5×10^{-4}	3.5×10^{-3}	1.4×10^{-2}
1	5	8.9×10^{-3}	6.9×10^{-2}	7.7×10^{-2}
1	10	6.6×10^{-4}	3.2×10^{-2}	5.5×10^{-2}
1	15	1.6×10^{-4}	1.7×10^{-2}	3.5×10^{-2}
1	20	1.5×10^{-4}	8.8×10^{-3}	2.6×10^{-2}
1	25	1.5×10^{-4}	4.9×10^{-3}	1.8×10^{-2}
1	30	1.5×10^{-4}	2.5×10^{-3}	1.1×10^{-2}

use a fourth-order explicit two-step method as our basic solver on a 200×100 uniform mesh. This provides a relative error less than 10^{-3} for $0 \leq t \leq 50$. The boundary conditions and/or layer equations were also approximated to fourth order. In all cases we compute the relative L_2 -errors on a uniform 50×25 mesh. Complete details on our discretization techniques will be given in Alpert *et al.* (1999a).

Padé approximants and generalizations

Results of these experiments are summarized in Table 2. I ran experiments with $p = 0 - 30$ and the initializations $\hat{R}_0 = 0$ and $\hat{R}_0 = 1$. The results are consistent with the error estimates. Generally, the largest errors occurred near $t = 50$, and we are unable to achieve an error at the level of the discretization error at this late time with $p \leq 30$. We are, on the other hand, fairly close to this goal at $t = 25$. The errors for the second sequence, $\hat{R}_0 = 1$, are generally slightly smaller than those obtained using the Padé sequence. This sequence also has the advantage of being exact at steady state. Finally we note that the short time error of 1.5×10^{-4} is the best one can do for the problem at hand and the mesh I have used. Indeed, it is the same error found if one uses the exact solution as a Dirichlet condition at the artificial boundary.

Table 3. *Uniform rational approximation coefficients, $\hat{K} \approx \sum_j \frac{\alpha_j}{s-\beta_j}$: $\tau = 10^{-3}$, $\eta = 10^{-4}$. Complex numbers are written in the form (real,imaginary)*

j	α_j	β_j
1,2	(-.2410467618025768E-6, \pm .2431987763837349E-6)	(-.4998142304334231E-4, \pm .9999998607359947)
3,4	(-.1617695923999794E-5, \pm .1638622585172068E-5)	(-.2501648855535112E-3, \pm .9999990907954994)
5,6	(-.7723476507531262E-5, \pm .7878743138182415E-5)	(-.8021925048752190E-3, \pm .9999958082358295)
7,8	(-.3400304516975200E-4, \pm .3510673092397324E-4)	(-.2263515963206483E-2, \pm .9999820162287431)
9,10	(-.1454893381589074E-3, \pm .1535469093409158E-3)	(-.6112737916031916E-2, \pm .9999224860282032)
11,12	(-.6104572904148162E-3, \pm .6733883694898616E-3)	(-.1625071664643320E-1, \pm .9996497460330479)
13,14	(-.2473202929583869E-2, \pm .3011442350813045E-2)	(-.4295328074381198E-1, \pm .9982864080633248)
15,16	(-.8964957513027030E-2, \pm .1398751873403249E-1)	(-.1129636068874967, \pm .9907617913485537)
17,18	(-.1846252520037211E-1, \pm .6565858806543060E-1)	(-.2902222956062986, \pm .9462036470847180)
19,20	(.9181095934161065E-1, \pm .2076825633238755)	(-.6548034445533449, \pm .7077228221122372)
21	(.3787484004895032,0)	(-.9345542777004186,0)

Table 4. *Errors using uniform rational approximant*

p	Max. err. $t \leq 5$	Max. err. $t \leq 25$	Max. err. $t \leq 50$
21	1.5×10^{-4}	4.1×10^{-4}	5.3×10^{-4}

Uniform approximants

For all Fourier modes we use the approximant determined by a tolerance of $\tau = 10^{-3}$ and an offset parameter of $\eta = 10^{-4}$. This yields a 21-pole approximation with parameters listed in Table 3. Note that for our mesh we certainly have $M \leq 100$ so that $\eta < (MT)^{-1}$. Hence the error due to the boundary condition is smaller than τ .

The results, summarized in Table 4, are very encouraging. For all time intervals considered, the accuracy is the best that can be obtained on the given mesh, as determined by using exact Dirichlet data at the boundaries. Given the modest number of poles used, the efficiency of this approach is unparalleled, as predicted by the complexity analysis.

We note that the data in this case was generously provided by Brad Alpert. More comprehensive experiments and detailed discussions of the numerical algorithms will be given in Alpert *et al.* (1999a).

Reflectionless sponge layer

Results of our experiments with the reflectionless sponge layer or PML are summarized in Table 5. I must admit from the outset that the great variety of possible layers, determined by different absorption profiles, widths, and local realizations, makes it difficult to claim that any particular experiment is definitive or comprehensive. Of interest in this regard is the paper of Turkel and Yefet (1998), where a variety of different formulations are compared for the same problem.

Equations (3.18)–(3.20) are discretized to fourth order, with an implicit treatment of the absorption terms. We use a quartic rather than the usual quadratic variation of σ . Periodic boundary conditions are used at the terminating point. Listed in the table are the maximum value of σ , which we varied between 10 and 80, and the total number of points in each layer, n_l , which we varied between 25 and 75. For values of σ_{\max} too large in comparison with the layer width, in particular for the 25 point layer and $\sigma_{\max} = 40, 80$, the solution grew and the errors became large. I do not list these results here.

The results of this experiment are in basic agreement with the error estimates. This can be verified by checking the ratio

$$\frac{d\bar{\sigma}}{\left(\ln \frac{1}{\tau} + \sqrt{\ln \frac{1}{\tau} \cdot T\bar{\sigma}}\right)}.$$

In absolute terms, however, the performance is somewhat disappointing. The best results are achieved for the thickest layer and $\sigma_{\max} = 40$, and almost reach the minimum possible error for $t \leq 5$. However, the long time results are worse than those obtained with the other methods. Improvements might be achieved by changing the discretization. I was unable to take σ very large, for fixed mesh spacing, without encountering asymptotic instabilities.

3.9. Approximations in the dissipative case

In the preceding sections we studied many well-developed techniques for approximating radiation boundary conditions in the hyperbolic case. In contrast, much less has been done for equations of mixed type. It is an interesting issue if the highly efficient rational approximants we shall consider can be extended to these cases. As the kernels to be approximated often involve the same analytic functions with arguments restricted to subdomains of the domains of interest in the hyperbolic case, one is tempted to conjecture that it is possible. However, there is the complicating factor that the transforms do not behave like rational functions at infinity.

For problems with small diffusion coefficients or viscosities, rational approximants in the spirit above have been proposed and analysed by Halpern (1986) for the scalar advection–diffusion equation, and by Halpern and

Table 5. *Errors using (3.17)*

σ_{\max}	n_l	Max. err. $t \leq 5$	Max. err. $t \leq 25$	Max. err. $t \leq 50$
10	25	3.0×10^{-1}	3.5×10^{-1}	4.3×10^{-1}
20	25	6.2×10^{-2}	1.9×10^{-1}	6.3×10^{-1}
10	50	5.0×10^{-2}	1.0×10^{-1}	1.0×10^{-1}
20	50	5.3×10^{-3}	6.1×10^{-2}	8.7×10^{-2}
40	50	7.7×10^{-4}	4.8×10^{-2}	1.7×10^{-1}
80	50	2.9×10^{-3}	1.4×10^{-1}	5.8×10^{-2}
10	75	8.0×10^{-3}	6.9×10^{-2}	7.4×10^{-2}
20	75	2.8×10^{-4}	3.2×10^{-2}	5.7×10^{-2}
40	75	2.0×10^{-4}	1.1×10^{-2}	4.3×10^{-2}
80	75	4.8×10^{-4}	2.9×10^{-2}	1.1×10^{-1}

Schatzman (1989) for the linearized incompressible Navier–Stokes equations. Error estimates in the small parameters are given.

It is also possible to make use of the special properties of dissipative problems to derive simple boundary conditions with some provable accuracy. One can exploit the differing decay rates of different modes to identify ‘dominant’ wave groups in the far field, and use boundary conditions that interpolate the exact conditions at these locations in wave number space. This procedure is developed in Hagstrom (1991*a*). Asymptotic error estimates are thereby derived, leading to an error, for planar boundaries, which decays in the general case like L^{-1} where L is domain length. In Hagstrom (1991*b*) these ideas are applied to the incompressible Navier–Stokes equations in a channel, producing conditions which seem reasonably accurate at moderate Reynolds numbers.

An interesting class of problems that can be accurately solved using simple boundary conditions are singularly perturbed hyperbolic systems at boundaries with no incoming characteristics. The simplest model of such a problem is the scalar advection–diffusion equation (2.43) at outflow ($U_1 > 0$) under the assumption $\nu \ll 1$. We then notice that the ‘incoming’ solution

$$\hat{u} = Ee^{\lambda_+ x}, \quad \lambda_+ = \frac{U_1 + \sqrt{U_1^2 + 4\nu(s + iU_{\tan} \cdot k + \nu|k|^2)}}{2\nu},$$

is of boundary layer type, as

$$\operatorname{Re} \lambda_+ \geq \frac{U_1}{2\nu} \gg 1.$$

Therefore, any error we make at the boundary very rapidly decays into the interior. From a numerical perspective, however, the boundary layer may lead to large errors for an unrefined mesh – and one certainly does not want to refine an unphysical boundary layer at an artificial boundary. The amplitude of the layer can be decreased through the use of extrapolation conditions. Namely, we impose

$$\frac{\partial^r u}{\partial x^r} = 0, \quad r \geq 1.$$

The error associated with this boundary condition can again be explicitly analysed. Using the exact solution near the boundary given in (2.44), we find that the error satisfies

$$\hat{e} = (-1)^r \left(\frac{4\nu(s + iU_{\text{tan}} \cdot k + \nu|k|^2)}{(U_1 + \sqrt{U_1^2 + 4\nu(s + iU_{\text{tan}} \cdot k + \nu|k|^2)})^2} \right)^r A e^{\lambda+x}.$$

Clearly, for $s + iU_{\text{tan}} \cdot k + \nu|k|^2$ not too large, the error is $O(\nu^r)$ and r x -derivatives are bounded independent of ν . In the large s , $|k|$ regime the prefactor is not small, but generally the solution amplitude, A , is exponentially small as its exponent has an $O(\nu^{-1})$ negative real part.

Precise arguments and error estimates, including general boundaries and variable coefficients, are given in Lohéac (1991). Nordström (1995), Nordström (1997) established the accuracy of extrapolation boundary conditions at supersonic outflow for the compressible Navier–Stokes system. Surprisingly these results are extended to the subsonic case, where there is an incoming characteristic, if there are large transverse solution gradients. This result is applicable when physical boundary layers intersect the artificial boundary. Extrapolation conditions can also be used for the incompressible Navier–Stokes equations as in Johansson (1993).

4. Conclusions and open problems

Our fundamental conclusion, amply demonstrated by the theory and fully supported by our as yet sparse numerical experimentation, is that the basic constant coefficient equations of wave theory on unbounded domains with sufficiently simple tails can be accurately solved at essentially the same cost as solving a standard problem on the bounded subdomain of interest. Excepting the case of computational domains of high aspect ratio, which I will discuss further below, the uniform rational approximants seem to provide an ideal solution. In particular, the work associated with their application is generally less than required by the interior solver. However, for spherical boundaries, direct implementations of the exact condition are only slightly less efficient, and, using the local form, extremely easy to implement. For short to moderate time calculations, local conditions based on high

degree Padé approximants or the use of reflectionless sponge layers are also acceptable.

Despite the remarkable progress made over the past few years, there are still many important problems which remain unsolved. Below I will mention those which I think are most important, along with some speculations concerning their possible solution.

High aspect ratio domains. For exterior problems, our best techniques require the use of a spherical artificial boundary. In the most extreme cases, for example, scattering from a body with two small dimensions such as a wire, we are required to use a computational domain whose volume is greater by a factor of the aspect ratio squared than the potential domain of interest. This is clearly undesirable. One possible solution for short to moderate times is to use a long cylindrical domain with simple boundary conditions at the ends, but such a procedure becomes inefficient as the time becomes large.

More desirable would be the development of efficient approximations to the exact boundary condition on a family of domains that include domains of high aspect ratio. The obvious candidates here are prolate and oblate spheroids, as the wave equation is separable in the associated coordinate system. From our point of view, the primary difference between this case and those we have treated is the lack of scale invariance of the boundary. This leads to the dependence on the Laplace transform parameter, s , of the angular eigenfunctions of the exact boundary operator. If we choose to expand in a fixed basis, such as the spherical harmonics, the temporally nonlocal part of the operator is no longer a diagonal matrix. Naturally, this complicates its approximation, but I do not believe that it precludes the existence of effective uniform approximants. Therefore, the detailed study of this operator seems worthwhile. A distinct approach to its elucidation and approximation may be via multipole expansions of the solution. We have seen that these may be used to express the exact condition on a sphere. They have recently been studied for frequency domain problems in the spheroidal case by Holford (1999).

Planar boundary conditions on a rectangular box. Another possibility for constructing high aspect ratio domains is the use of rectangular boxes and either the Padé approximants or a reflectionless sponge layer. In light of the bad long time behaviour of our error estimates and computational experiments on periodic domains, this would seem an unlikely solution. However, there are suggestive arguments that better estimates might hold on box domains. Therefore, I believe that a rigorous error analysis for these boundary conditions on boxes should be developed.

Anisotropic systems in exterior domains. As mentioned in our discussion of the linearized compressible Euler equations, we have no general construction of exact boundary conditions for anisotropic problems on bound-

aries which include characteristic points. Of course a general theory, which might be based on the Riemann function, would be most desirable. Failing that, a particular solution in the gas dynamics case would have many applications. Such a solution would probably follow easily from the construction of exact conditions for the convective wave equation.

Approximation of exact conditions for problems of mixed order.

As we have seen, it is straightforward to develop expressions for exact boundary conditions in these cases. However, the associated theory of rational approximations is essentially undeveloped. Progress on this front could be very useful, particularly for nondissipative problems such as equations of Schrödinger or Boussinesq type.

Variable coefficients. Many important problems in wave theory involve propagation in inhomogeneous media. Examples include aeroacoustics, underwater acoustics, and seismics. Unfortunately, the theory as now developed says little about such problems, except in some very special cases mentioned above. A natural starting point is the wave equation in a stratified medium. A reasonable program is to characterize the exact boundary condition and attempt to construct approximations. However, this will again be a case where the eigenfunctions of the exact operator will depend on the Laplace transform parameter, so it is not clear how far one can go with our most successful approach. It may prove easier to construct reflectionless sponge layers, but this is again an open question.

It is worth remembering that some of the earliest work on numerical radiation boundary conditions, namely Engquist and Majda (1977, 1979), made use of geometrical optics and, hence, was naturally extensible to variable coefficients. The existence of a limiting operator could even be proven. However, the use of this theory to characterize the accuracy, as carried out by Halpern and Rauch (1987), depends on the assumption that the wave field is dominated by high frequencies. An intriguing alternative, suggested by the results of Radvugin and Zaitsev (1998), is to use a coordinate system in the exterior which is characteristics-based in the hope it will allow for a significant coarsening of the mesh and, hence, extension of the computational domain. Geometrical optics again seems the logical tool for assessing this approach.

In comparison with the problems mentioned above, I believe that a satisfactory general treatment of problems with variable coefficients will prove to be the most difficult. Nonetheless, good results just for some special cases, such as stratified media or perturbations thereof, would be quite useful.

REFERENCES

- S. Abarbanel and D. Gottlieb (1997), 'A mathematical analysis of the PML method', *J. Comput. Phys.* **134**, 357–363.
- M. Abramowitz and I. Stegun, eds (1972), *Handbook of Mathematical Functions*, Dover, New York.
- B. Alpert, L. Greengard and T. Hagstrom (1999a), 'Accurate solution of the wave equation on unbounded domains'. In preparation.
- B. Alpert, L. Greengard and T. Hagstrom (1999b), 'Rapid evaluation of nonreflecting boundary kernels for time-domain wave propagation', *SIAM J. Numer. Anal.* To appear.
- C. R. Anderson (1992), 'An implementation of the fast multipole method without multipoles', *SIAM J. Sci. Statist. Comput.* **13**, 923–947.
- A. Barry, J. Bielak and R. MacCamy (1988), 'On absorbing boundary conditions for wave propagation', *J. Comput. Phys.* **79**, 449–468.
- A. Bayliss and E. Turkel (1980), 'Radiation boundary conditions for wave-like equations', *Comm. Pure Appl. Math.* **33**, 707–725.
- J.-P. Berenger (1994), 'A perfectly matched layer for the absorption of electromagnetic waves', *J. Comput. Phys.* **114**, 185–200.
- P. Bettess (1992), *Infinite Elements*, Penshaw Press, Sunderland, UK.
- W. Chew and W. Weedon (1994), 'A 3-D perfectly matched medium from modified Maxwell's equations with stretched coordinates', *Microwave Optical Technol. Lett.* **7**, 599–604.
- F. Collino (1993), Conditions d'ordre élevé pour des modèles de propagation d'ondes dans des domaines rectangulaires, Technical Report 1790, INRIA.
- F. Collino and P. Monk (1998), 'Optimizing the perfectly matched layer'. Preprint.
- L. Demkowicz and K. Gerdes (1999), 'Convergence of the infinite element methods for the Helmholtz equation in separable domains', *Numer. Math.* To appear.
- G. Doetsch (1974), *Introduction to the Theory and Application of the Laplace Transformation*, Springer, New York.
- J. Driscoll, D. Healy and D. Rockmore (1997), 'Fast discrete polynomial transforms with applications to data analysis for distance transitive graphs', *SIAM J. Comput.* **26**, 1066–1099.
- B. Engquist and A. Majda (1977), 'Absorbing boundary conditions for the numerical simulation of waves', *Math. Comput.* **31**, 629–651.
- B. Engquist and A. Majda (1979), 'Radiation boundary conditions for acoustic and elastic wave calculations', *Comm. Pure Appl. Math.* **32**, 313–357.
- A. Eringen and E. Şühubi (1975), *Elastodynamics*, Vol. 2, Academic Press, New York.
- T. Geers (1998), Benchmark problems, in *Computational Methods for Unbounded Domains* (T. Geers, ed.), Kluwer Academic Publishers, Dordrecht, Netherlands, pp. 1–10.
- M. Giles (1990), 'Nonreflecting boundary conditions for Euler equation calculations', *AIAA Journal* **28**, 2050–2058.
- D. Givoli (1991), 'Non-reflecting boundary conditions', *J. Comput. Phys.* **94**, 1–29.
- D. Givoli (1992), *Numerical Methods for Problems in Infinite Domains*, Vol. 33 of *Studies in Applied Mechanics*, Elsevier, Amsterdam.

- D. Givoli and D. Kohen (1995), 'Non-reflecting boundary conditions based on Kirchoff-type formulae', *J. Comput. Phys.* **117**, 102–113.
- J. Goodrich and T. Hagstrom (1999), 'High-order radiation boundary conditions for computational aeroacoustics'. In preparation.
- L. Greengard and P. Lin (1998), 'On the numerical solution of the heat equation on unbounded domains (Part I)'. Preprint.
- L. Greengard and V. Rokhlin (1997), A new version of the fast multipole method for the Laplace equation in three dimensions, in *Acta Numerica*, Vol. 6, Cambridge University Press, pp. 229–269.
- M. Grote and J. Keller (1995), 'Exact nonreflecting boundary conditions for the time dependent wave equation', *SIAM J. Appl. Math.* **55**, 280–297.
- M. Grote and J. Keller (1996), 'Nonreflecting boundary conditions for time dependent scattering', *J. Comput. Phys.* **127**, 52–81.
- M. Grote and J. Keller (1998), Exact nonreflecting boundary conditions for elastic waves, Technical Report 1998-08, ETH, Zürich.
- M. Grote and J. Keller (1999), 'Nonreflecting boundary conditions for Maxwell's equations', *J. Comput. Phys.* To appear.
- B. Gustafsson and H.-O. Kreiss (1979), 'Boundary conditions for time-dependent problems with an artificial boundary', *J. Comput. Phys.* **30**, 333–351.
- T. Hagstrom (1983), Reduction of Unbounded Domains to Bounded Domains for Partial Differential Equation Problems, PhD thesis, California Institute of Technology.
- T. Hagstrom (1991a), 'Asymptotic boundary conditions for dissipative waves: General theory', *Math. Comput.* **56**, 589–606.
- T. Hagstrom (1991b), 'Conditions at the downstream boundary for simulations of viscous, incompressible flow', *SIAM J. Sci. Statist. Comput.* **12**, 843–858.
- T. Hagstrom (1995), On the convergence of local approximations to pseudodifferential operators with applications, in *Proc. 3rd Int. Conf. on Math. and Num. Aspects of Wave Prop. Phen.* (E. Bécache, G. Cohen, P. Joly and J. Roberts, eds), SIAM, pp. 474–482.
- T. Hagstrom (1996), On high-order radiation boundary conditions, in *IMA Volume on Computational Wave Propagation* (B. Engquist and G. Kriegsmann, eds), Springer, New York, pp. 1–22.
- T. Hagstrom and J. Goodrich (1998), 'Experiments with approximate radiation boundary conditions for computational aeroacoustics', *Appl. Numer. Math.* **27**, 385–402.
- T. Hagstrom and S. Hariharan (1996), Progressive wave expansions and open boundary problems, in *IMA Volume on Computational Wave Propagation* (B. Engquist and G. Kriegsmann, eds), Springer, New York, pp. 23–43.
- T. Hagstrom and S. Hariharan (1998), 'A formulation of asymptotic and exact boundary conditions using local operators', *Appl. Numer. Math.* **27**, 403–416.
- T. Hagstrom and H. B. Keller (1986), 'Exact boundary conditions at an artificial boundary for partial differential equations in cylinders', *SIAM J. Math. Anal.* **17**, 322–341.
- T. Hagstrom and J. Lorenz (1994), Boundary conditions and the simulation of low Mach number flows, in *Proceedings of the First International Conference on*

- Theoretical and Computational Acoustics* (D. Lee and M. Schultz, eds), World Scientific, Singapore, pp. 657–668.
- E. Hairer, C. Lubich and M. Schlichte (1985), ‘Fast numerical solution of nonlinear Volterra convolutional equations’, *SIAM J. Sci. Statist. Comput.* **6**, 532–541.
- L. Halpern (1986), ‘Artificial boundary conditions for the linear advection diffusion equation’, *Math. Comput.* **46**, 425–438.
- L. Halpern (1991), ‘Artificial boundary conditions for incompletely parabolic perturbations of hyperbolic systems’, *SIAM J. Math. Anal.* **22**, 1256–1283.
- L. Halpern and J. Rauch (1987), ‘Error analysis for absorbing boundary conditions’, *Numer. Math.* **51**, 459–467.
- L. Halpern and J. Rauch (1995), ‘Absorbing boundary conditions for diffusion equations’, *Numer. Math.* **71**, 185–224.
- L. Halpern and M. Schatzman (1989), ‘Artificial boundary conditions for viscous incompressible flows’, *SIAM J. Math. Anal.* **20**, 308–353.
- S. He and V. Weston (1996), Wave-splitting and absorbing boundary conditions for Maxwell’s equations on a curved surface, Technical Report TRITA-TET-96-14, KTH, Stockholm.
- R. Higdon (1986), ‘Absorbing boundary conditions for difference approximations to the multidimensional wave equation’, *Math. Comput.* **47**, 437–459.
- R. Higdon (1987), ‘Numerical absorbing boundary conditions for the wave equation’, *Math. Comput.* **49**, 65–90.
- R. Higdon (1991), ‘Absorbing boundary conditions for elastic waves’, *Geophysics* **56**, 231–254.
- R. Higdon (1992), ‘Absorbing boundary conditions for acoustic and elastic waves in stratified media’, *J. Comput. Phys.* **101**, 386–418.
- R. Higdon (1994), ‘Radiation boundary conditions for dispersive waves’, *SIAM J. Numer. Anal.* **31**, 64–100.
- R. Holford (1999), ‘A multipole expansion for the acoustic field exterior to a prolate or oblate spheroid’. Submitted to *J. Acoust. Soc. Amer.*
- C. Johansson (1993), ‘Boundary conditions for open boundaries for the incompressible Navier–Stokes equations’, *J. Comput. Phys.* **105**, 233–251.
- T. Kato (1976), *Perturbation Theory for Linear Operators*, Springer, New York.
- H.-O. Kreiss and J. Lorenz (1989), *Initial-Boundary Value Problems and the Navier–Stokes Equations*, Academic Press, New York.
- E. Lindman (1975), ‘Free space boundary conditions for the time dependent wave equation’, *J. Comput. Phys.* **18**, 66–78.
- J.-P. Lohéac (1991), ‘An artificial boundary condition for an advection-diffusion equation’, *Math. Meth. Appl. Sci.* **14**, 155–175.
- D. Ludwig (1960), ‘Exact and asymptotic solutions of the Cauchy problem’, *Comm. Pure Appl. Math.* **13**, 473–508.
- M. Mohlenkamp (1997), ‘A fast transform for spherical harmonics’. Preprint.
- R. Newton (1966), *Scattering Theory of Waves and Particles*, McGraw-Hill, New York.
- J. Nordström (1995), ‘Accurate solutions of the Navier–Stokes equations despite unknown outflow boundary data’, *J. Comput. Phys.* **120**, 184–205.

- J. Nordström (1997), 'On extrapolation procedures at artificial outflow boundaries for the time-dependent Navier–Stokes equations', *Appl. Numer. Math.* **23**, 457–468.
- F. Oberhettinger and L. Badii (1970), *Tables of Laplace Transforms*, Springer, New York.
- F. Olver (1954), 'The asymptotic expansion of Bessel functions of large order', *Philos. Trans. Royal Soc. London* **A247**, 328–368.
- P. Petropoulos (1999), 'Reflectionless sponge layers as absorbing boundary conditions for the numerical solution of Maxwell's equations in rectangular, cylindrical and spherical coordinates'. Submitted to *SIAM J. Appl. Math.*
- Y. Radvogin and N. Zaitsev (1998), Absolutely transparent boundary conditions for time-dependent wave problems, in *Seventh International Conference on Hyperbolic Problems*.
- A. Ramm (1986), *Scattering by Obstacles*, D. Reidel, Dordrecht, Netherlands.
- V. Rokhlin (1990), 'Rapid solution of integral equations of scattering theory in two dimensions', *J. Comput. Phys.* **86**, 414–439.
- V. Ryabenkii (1985), 'Boundary equations with projections', *Russian Math. Surveys* **40**, 147–183.
- M. Schwartz (1987), *Principles of Electrodynamics*, Dover, New York.
- I. Sofronov (1993), 'Conditions for complete transparency on the sphere for the three-dimensional wave equation', *Russian Acad. Sci. Dokl. Math.* **46**, 397–401.
- I. Sofronov (1999), 'Artificial boundary conditions of absolute transparency for two- and three-dimensional external time-dependent scattering problems', *Euro. J. Appl. Math.* To appear.
- L. Ting and M. Miksis (1986), 'Exact boundary conditions for scattering problems', *J. Acoust. Soc. Amer.* **80**, 1825–1827.
- L. Trefethen and L. Halpern (1986), 'Well-posedness of one-way wave equations and absorbing boundary conditions', *Math. Comput.* **47**, 421–435.
- L. Trefethen and L. Halpern (1988), 'Wide-angle one-way wave equations', *J. Acoust. Soc. Amer.* **84**, 1397–1404.
- S. Tsynkov (1998), 'Numerical solution of problems on unbounded domains. A review', *Appl. Numer. Math.* **27**, 465–532.
- E. Turkel and A. Yefet (1998), 'Absorbing PML boundary layers for wave-like equations', *Appl. Numer. Math.* **27**, 533–557.
- O. Vacus (1996), Singularités de frontière et conditions limites absorbantes: le problème du coin, Technical Report 2851, INRIA.
- L. Xu and T. Hagstrom (1999), 'On convergent sequences of approximate radiation boundary conditions and reflectionless sponge layers'. In preparation.